

Contents lists available at ScienceDirect

European Journal of Pharmaceutics and Biopharmaceutics

journal homepage: www.elsevier.com/locate/ejpb





Novel electrosprayed core-shell polyethyleneimine and phospholipid coated MSNs for Co-delivery of KAZ3 and MDR-1 siRNA for efficient chemotherapy in multidrug-resistant colon cancer

Elshaimaa Sayed ^{a,b}, Ketan Ruparelia ^a, Saman Zafar ^c, Ahmed Faheem ^{d,e}, Dimitris Fatouros ^{f,g}, Muhammad Sohail Arshad ^{c,*}, Neenu Singh ^{a,h}, Zeeshan Ahmad ^{a,i,**}

- ^a Leicester School of Pharmacy, De Montfort University, Leicester, United Kingdom
- ^b Department of Pharmaceutics, Faculty of Pharmacy, Minia University, Minia, Egypt
- ^c Faculty of Pharmacy, Bahauddin Zakariya University, Multan, Pakistan
- d School of Pharmacy and Pharmaceutical Sciences, Faculty of Health Sciences and Wellbeing, University of Sunderland, Sunderland, United Kingdom
- ^e Faculty of Pharmacy, University of Tanta, Tanta, Egypt
- Department of Pharmaceutical Technology, School of Pharmacy, Faculty of Health Sciences, Aristotle University of Thessaloniki, Thessaloniki, Greece
- g Center for Interdisciplinary Research and Innovation (CIRI-AUTH), Thessaloniki, Greece
- ^h School of Allied Health Sciences, De Montfort University, Leicester, United Kingdom
- ⁱ Division of Pharmacy and Optometry, School of Health Sciences, University of Manchester, United Kingdom

ARTICLE INFO

Keywords: EHDA Electrospray Coaxial Particle Coating Drug delivery Co-therapy

ABSTRACT

Different strategies and multifunctional nano-carriers have been employed to enhance chemotherapeutic drugs bioavailability and tackle acquired multi-drug resistance (MDR) thus ensuring efficient chemotherapy with fewer adverse effects. Among these, mesoporous Silica Nanoparticles (MSNs) are exciting matrices for improving cytotoxic drugs bioavailability and circumventing MDR through its potential of co-delivery of anticancer agents and short interfering RNA (siRNA).

In this study, Mons were coated with (1:1) Polyethyleneimine (PEI) and phospholipids (PL) composite and were loaded with KAZ3 (Anticancer chalcone) using coaxial electrospraying in a one step process. The novel delivery system was used to co-deliver both MDR-1 siRNA and KAZ3 to colon cancer cell lines in order to knockdown the MDR-1 gene and thus to improve KAZ3 cytotoxicity. The prepared drug/siRNA delivery system was characterized using SEM, fluorescence microscopy, TGA, zeta sizer, actives (KAZ3 and siRNA) loading efficiency, actives release studies, siRNA gel retardation and actives cellular uptake. The cytotoxicity of formulations against cancer cell lines (HCT 116) was also assessed using MTT assay and MDR-1 gene silencing efficiency using western blotting. Results showed that coaxial electrospraying was efficient in preparing coreshell coated MSNs that were able to co-deliver both MDR-1 siRNA and KAZ3 to colon cancer lines. The MSNs coated with PL and 2.5 KDa PEI were found to be more compatible with human cells than to 25KDa PEI coated MSNs. KAZ3/siRNA loaded PEI-PL coated MSNs were successful in decreasing multidrug resistance gene expression to 40 % and causing up to 92 % colon cancer cell death. The findings of the present study show the immense potential of electro-hydrodynamic atomization (EHDA) as a technique for producing drug loaded MSNs based core-shell particles.

1. Introduction

Although cancer therapy adopts different clinical strategies that include chemotherapy, radiation and surgery, chemotherapy remains the ideal choice for cancer treatment. Chemotherapy uses cytotoxic

drugs that inhibit cancer cells division and tumour growth. Patients treated with chemotherapy demonstrated improved survival rate [1,2]. However, cancer treatment using conventional chemotherapy faces major obstacles such as unselective cytotoxicity, acquired MDR, poor aqueous solubility, low permeability and poor bioavailability of most

 $^{^{\}star}\ Corresponding\ author\ at:\ Faculty\ of\ Pharmacy,\ Bahauddin\ Zakariya\ University,\ Multan,\ Pakistan.$

^{**} Corresponding author at: Division of Pharmacy and Optometry, School of Health Sciences, University of Manchester, United Kingdom. E-mail addresses: sohailarshad@bzu.edu.pk (M.S. Arshad), zahmad@dmu.ac.uk, zeeshan.ahmad@manchester.ac.uk (Z. Ahmad).

cytotoxic drugs [2–5]. Long periods of chemotherapy cause cancer cells to develop different resistance mechanisms (e.g. pump and non-pump resistance) simultaneously against variety of drugs that are functionally and structurally unrelated [4]. Multidrug resistant cells are able to pump cytotoxic drugs out of the cellular cytoplasm *via* adenosine triphosphate-binding cassette (ABC) membrane transporters such as P-gp (i.e. MDR-1, ABCB1). These efflux pumps are activated upon drug molecules exposure, lowering the concentration of cytotoxic agent in the cytoplasm [6]. As a result, a failure of chemotherapy occurs and thus a higher and a frequent dosage regimen of cytotoxic drugs is required. Consequently, increased cytotoxic adverse effects against healthy tissues are expected [5,6]. Therefore, different approaches have been employed to tackle MDR, to enhance chemotherapeutic drugs bioavailability, decrease their adverse effects and hence to ensure efficient chemotherapy [6,7].

MSNs are emerging as a smart nanotechnology for efficient anticancer drug delivery and as a promising route for successful cancer therapy [4,8-10]. MSNs are able to enhance inherent properties of cytotoxic drugs (e.g. solubility and permeability) [9], deliver them to the tumor site and ensure their internalization into cancer cells cytosol [11]. Additionally, these nanocarriers are able to overcome MDR through their unique ability to co-deliver anticancer agents with MDR modulators such as tetrandrine [12] or MDR silencing siRNA [11,13]. siRNA is transfected to cancer cells in order to silence genes responsible for MDR thus enhancing cytotoxic drugs cellular uptake, exerting synergistic apoptotic effect and reducing tumour growth [13-15]. Loading large biological molecules such as siRNA inside MSNs mesopores (typically 2-10 nm) is not straightforward, therefore siRNA molecules are preferred to be attached to MSNs external surfaces with aid of cationic polymer shell such as polyethyleneimine (PEI) [16-19]. This core-shell design has the advantage of leaving the mesoporous core of MSNs accessible to accommodate large amounts of anticancer drugs allowing the co-delivery strategy [19,20].

Polyethyleneimine (PEI) has proven to be one of the most effective polymers for nucleic acid delivery due to its greater ability to condense RNA or DNA (polyplexes formation) and release them inside the cytoplasm through its endosomal escape property [21,22]. PEI owns a high pH buffering capacity due to its ability to accumulate protons inside the endosomes allowing endosomal osmotic rupture, which then triggers the polyplexes escape into cytosol protecting them from lysosomal degradation. This phenomenon known as a 'proton sponge effect' and is certainly crucial for efficient gene transfection [19,23]. The PEI capacity to bind to nucleic acid and the polyplex formation are greatly affected by nitrogen/phosphate (N/P) ratio. It is a chief parameter that significantly affects transfection efficiency in gene delivery. N/P ratio is described as the simple ratio of the number nitrogen atoms in PEI to the number of phosphate atoms in siRNA [24].

High molecular weight (MW) PEI is well known for its high toxicity which is attributed to its high positive charge density which depolarises the mitochondrial membranes thus hindering its *in-vivo* applications. In contrast, low MW PEI is more biocompatible with minimal toxicity but with lower gene trafficking and silencing abilities [25,26]. Different approaches have been investigated to accomplish the balance between cytotoxicity and transfection efficiency of PEI, including complexation of low MW PEI with PEG [11], hydrophobic modification of PEI [26] or conjugation with phospholipids (PL) moieties [25,27,28]. Studies demonstrated that (1:1) PL substitution of PEI attained better protection and condensation of siRNA [25,27,28]. PEI-lipid composites were shown to offer an improved interaction with the cell membrane resulting in enhanced cellular gene transfection, better biocompatibility and longer circulation time [27,28].

Electrohydrodynamic atomisation (EHDA), which includes (but not limited to) electrospraying and electrospinning, is considered a versatile, simple and flexible technique for the preparation of nano- and micro-particulate/fibrous/porous materials which are used in a wide range of pharmaceutical and biomedical applications [29–37].

Furthermore, the EHDA process permits formulation material properties to dictate the end product; permitting controlled engineering of shape, size and even multi-material composites [38–42]. Although more timely advances have focused on adapting these processes to 3D printing [43–45], many of the core advantages of this emerging method remain to be fully exploited as comparative atomisation technologies [46]. This atomisation approach has been used to coat, fabricate or load micro- or nano-particles [29].

Coating of particles enables functionalities e.g., modifying the hydrophilic or hydrophobic behaviour or catalytic activity. In addition, coating of particles is of great interest for diagnostic applications and targeted drug delivery. Dry and solvent based techniques have been used to coat particles. In the former approach, the difficulty lies in dispersing dry particles for coating. In the latter technique, solvent removal, additional drying and dispersion steps are required because the product is produced in a liquid medium [47]. The EHDA technique, involving break-up of a liquid jet under influence of electrical forces, overcomes these drawbacks and offers unique advantages e.g., narrow droplet size distribution and self-dispersing of unipolarly droplets. Electrospraying of polymeric solution results in a charged spray which overcomes the difficulty in dispersing and depositing particles on host nanoparticles. Once coated, van der Waals forces hinder detachment of guest particulates from host particles [46,47]. Other key advantages associated with the EHDA approach include precise control over droplet size, morphology and coating thickness, ease of scale-up, high throughout and low shear stress [29,38].

In our previous research study, we have demonstrated the feasibility of electrospraying as a novel technique to load mesoporous silica with the poorly water-soluble anticancer drug (KAZ3). The electrosprayed formulations exhibited improved dissolution rates and enhanced permeability across rat intestine [9].

In the present study, we have adopted two novel strategic plans; processing strategy and material strategy. To the best of our knowledge, this is amongst the earliest reports where electrospraying is used to load active as well as coat MSNs simultaneously; all in a single step. Other studies have performed the loading and coating procedures in more than one process; MSNs phosphonate surface modification to increase the negativity of their surface in order to enable the electrostatic interaction with the cationic polymer, PEI polymer coating and finally loading actives into the coated MSNs [18,48]. Each one of these processes is a multistep complex procedure that is time and cost consuming.

In terms of material strategy, MCM-41-type MSNs coated with a composite of low MW PEI (2.5 K) and PLs (phosphatidylcholine (PC) or Dioleoyl phosphatidylethanolamine (DOPE)) were utilized for the first time as a gene vector and drug carrier. This composite was used in order to improve the gene transfection ability of low MW PEI while keeping a reduced toxicity profile. The particle toxicity and gene transfection ability of the composite coated MSNs were determined and compared with those of PEI 25 K coated MSNs. The 2.5 k PEI and PLs coated MSNs showed better toxicity profiles and similar transfection ability to 25 K PEI coated MSNs.

Furthermore, we also show the electrosprayed products to co-deliver KAZ3 and MDR-1 siRNA to HCT-116 colon cancer cell lines in order to down regulate the multidrug resistance gene and to enhance KAZ3 cytotoxicity. KAZ3 loaded PEI-PL coated MSNs were characterized by means of scanning electron microscopy (SEM), thermogravimetric analysis (TGA), ζ -potential studies, actives (KAZ3 and siRNA) loading efficiency and release studies, siRNA gel retardation and cytocompatibility studies. Complementary analyses were performed by cellular uptake and gene silencing ability studies.

2. Materials and methods

2.1. Materials

MCM-41-type MSNs were purchased from Nanografi

Nanotechnology Co. Ltd (Ankara, Turkey). PEI MW 2.5 KD and 25 KD were from Polysciences Europe GmbH (Hirschberg, Germany). Phospholipids (PLs); Phosphatidylcholine (PC) and 1,2-Dioleoyl-sn-glycero-3-phosphoethanolamine (DOPE) were kindly granted from Lipoid GmbH (Ludwigshafen, Germany). HCT 116 colorectal cancer cell line was purchased from American Type Culture Collection (ATCC) (Gaithersburg, Maryland, USA). Acetone, ethanol, DMSO, human MDR-1 siRNA silencer® select, silencer Select negative control siRNA, silencer Cy™3-labeled Negative Control siRNA, ultraPure agarose, blue Juice gel loading buffer (10X), Novex Tris-borate-EDTA buffer (TBE) 5X and SYBRTM Safe Gel Stain, cell culture medium (Modified McCoy's 5A), TrypLE express enzyme and fetal bovine serum (FBS) were purchased from Themofisher scientificTM (Loughborough, UK). RNase free water from Alfa Aesar (Lancashire, UK). Protein inhibitor cocktail, BSA, MTT reagent were obtained from sigma aldrich (Dorset, UK), Dithiothreitol (DTT), ECL Substrate and Bradford bio-rad protein assay kit were obtained from Bio-rad (Hertfordshire, UK). RIPA Buffer, protein marker, anti-rabbit horseradish peroxidase (HRP)-linked antibody and rabbit antibodies against human MDR-1 and β-actin were supplied from cell signalling technology (London, UK). All reagents were analytical grade and used without further purification.

2.2. KAZ3 loading and PEI-PL coating of MSNs using electrospraying technology

KAZ3 laden PEI-PL coated MSNs were prepared using two electrospraying technologies namely; co-axial electrospraying techniques and single needle electrospraying.

Co-axial electrospraying was performed using MSNs dispersion (10 mg/mL) in KAZ3 acetone solution as the inner core, and ethanol solution of 1:1 mixture of 2.5 KDa PEI and PL (PC or DOPE) was used as the external shell. For comparison, ethanol solution of 25 KDa PEI or 2.5 KD PEI was also used as an external shell in two formulations. The above mixtures were separately loaded into 5 mL syringes that were attached to two individual infusion pumps (Harvard apparatus, USA). The pumps were connected into a spraying nozzle that comprised of two concentric (central and external) stainless steel needles through silicone tubing. MSNs or MSNs/KAZ3 suspensions (25 % w/w KAZ3) were infused into the internal capillary at an infusion rate of 25 μL /min. While the flow rate of the external PEI-PL solution was 50 μ L/min or 25 μ L/min. The mixtures were electrosprayed when an electric field of 15-17 kV was applied to the stainless-steel nozzle using a high-power supply (Genvolt high voltage power supply, UK). The electrosprayed particles were deposited onto a glass substrate.

For comparison purposes, a single needle electrospraying was also carried out under the same conditions using MSNs dispersion (10 mg/mL) in KAZ3, 2.5 KD PEI and PL (PC or DOPE, 5 mg/mL) ethanol

solution. The suspension was electrosprayed at a flow rate of (25 $\,\mu L/$ min) and applied voltage of (15–17 kV) through the inner stainless-steel needle. The composition of the different formulations and the used coating method are illustrated in Table 1.

2.3. Microscopic imaging

2.3.1. Scanning electron microscope (SEM)

The morphology of the electrosprayed formulations was examined using SEM (Carl Zeiss, Germany). The formulations were mounted on aluminium stubs using a double adhesive tape. The particles were coated with 10 nm gold using sputter coater (Edwards S150B, UK) and were then scanned at 10 kV accelerating voltage.

2.3.2. Fluorescence microscopy

The KAZ3 loaded coated MSNs were conjugated with Cy3-labeled siRNA (at N/P ratio 3, conjugation procedure is discussed in detail later in section 2.9). The core shell morphology of coated MSNs was investigated using fluorescence microscopy. The electrosprayed particles were mounted onto glass slides and imaged using fluorescence microscope (InvitrogenTM EVOS, UK). KAZ3 green fluorescence was captured at GFP channel (excitation/emission; 470/525 nm) while Cy3-labeled siRNA fluorescence was imaged at RFP channel (excitation/emission; 531/593 nm). The obtained images were then overlayed together.

2.4. Particle size and zeta potential measurement

The particle size distributions and ζ -potential of empty and coated MSNs formulations were investigated using laser NanoBrook Omni diffraction size and zeta analyser (Brookhaven, UK). Suspensions of one mg of each formulation in 2 mL phosphate buffer saline (PBS) were sonicated for 10 min prior to measurements. The measurements were conducted using a refractive index of 1.45 for the silica particles and 1.334 for the PBS dispersant. The particle size and ζ -potential measurements were repeated five times, and the average and standard deviation were calculated.

2.5. Determining PEI-PL coating percentage using thermogravimetric analysis (TGA)

The thermal behaviour of MSNs, PEI, DOPE, PC and unloaded coated formulations were obtained using Perkin Elmer Thermogravimeric analyzer (Pyris, US). 5–7 mg Samples were placed in porcelain pans and were heated in nitrogen at a heating rate of $10\,^{\circ}$ C/min from 20 to $800\,^{\circ}$ C. The obtained thermograms were used to determine the percent of PEI-PL coating in MSNs using the following equation:

Table 1
Composition, electrospraying method and quantification of KAZ3 encapsulation efficiency (EE %) of the different formulations calculated by UV spectrophotometry.

Formulation	PEI type and concentration	PL type and concentration	Electrospraying method	flow rate(s)	KAZ3 (EE%)	
K-MSNs	Uncoated	Uncoated	Single needle	25 μL/min	$91.3~\% \pm 3.1$	
MSNs -PEI-PC-SN	2.5 KDa PEI 2.5 mg/mL	PC 2.5 mg/mL	Single needle	25 μL/min	$88.5~\% \pm 11.6$	
MSNs- PEI-DOPE-SN	2.5 kDa PEI	DOPE	Single needle	25 μL/min	$94.6 \% \pm 14.3$	
	2.5 mg/mL	2.5 mg/mL				
MSNs-PEI-PC-CO	2.5KDa PEI	PC	Coaxial	Inner (MSNs): 25 μL/min	89.0 ± 4.6	
	1.25 mg/mL	1.25 mg/mL		Outer (PEI-PL): 50 µL/min		
MSNS-PEI-DOPE-CO	2.5 kDa PEI	DOPE	Coaxial	Inner (MSNs): 25 μL/min	$90.8~\%\pm0.3$	
	1.25 mg/mL	1.25 mg/mL		Outer (PEI-PL): 50 µL/min		
MSNs-PEI-CO	2.5 KDa PEI	None	Coaxial	Inner (MSNs): 25 µL/min	$66.6~\% \pm 2.4$	
	2.5 mg/mL			Outer (2.5 K PEI): 50 μL/min		
MSNs-25KDa PEI-CO	25 KDa PEI	None	Coaxial	Inner (MSNs): 25 µL/min	$70.9~\% \pm 4.8$	
	2.5 mg/mL			Outer (25 k PEI): 50 µL/min		
MSNs-PEI-PC-EFCO	2.5KDa PEI	PC	Coaxial	Inner (MSNs): 25 μL/min	$87.9 \% \pm 4.9$	
	2.5 mg/mL	2.5 mg/mL	5 mg/mL		nin	

PC: phosphatidylcholine, DOPE: Dioleoyl phosphatidylethanolamine, PEI: 2.5 KDa polyethyleneimine, 25KDa PEI: 25 KDa polyethyleneimine, SN: single needle electrospraying, CO: coaxial electrospraying and EFCO: equal flow rates coaxial electrospraying.

$$\label{eq:pein} \begin{split} \textit{PEI-PLCoating} \textit{percentage} &= \text{\%Wt.loss} \textit{of coated samples} \textit{from} (100\\ &- 800^{\circ}\text{C}) - \text{\%wtloss} \textit{of MSNs} \textit{from} (100\\ &- 800^{\circ}\text{C}) \end{split}$$

The PEI content was taken as half the total amount of coating since the coating mixture was used in ratio 1:1.

2.6. Differential scanning calorimetry (DSC)

DSC thermograms of pristine materials (KAZ3, MSNs, DOPE, PC, PEI) and KAZ3 loaded formulations were recorded using DS calorimeter (Perkin Elmer, US) from 25 to 350 $^{\circ}$ C at a heating rate of 10 $^{\circ}$ C/min under a nitrogen gas stream of 20 mL/min.

2.7. Powder X-ray diffraction (XRD)

The crystallinity of drug loaded formulations was analysed with Cu K α 1 radiation ($\lambda=1.54$ Å) using a D8-Advance diffractometer (Bruker, USA). Scattering angle were measured between 8° to 35° at a 0.03° step size.

2.8. Contact angles measurements

Water contact angles on bare MSNs and PEI-PL coated MSNs were measured using a sessile drop profile by an optical tensiometer (Theta Lite, Biolin Scientific, Sweden). A water drop of approximately 5 μL was deposited using a liquid manual dispenser (Hamilton syringe with a 22-gauge needle) on a smooth, homogenous surface. The images of the drop were taken at different time intervals. The contact angles were measured on both sides of the sessile drop, and the average was calculated as the result.

2.9. KAZ3 encapsulation efficiency (EE%) and in-vitro release study

To measure the EE%, 5 mg of the drug loaded electrosprayed formulations were suspended into 10 mL acetone and were sonicated for 30 min. The suspensions were centrifuged, and 1 mL of the supernatant was further diluted by acetone to 10 mL. The absorbance of the final diluted solutions was measured at $\lambda_{\rm max}$ 341 nm using UV spectrophotometry (Themo scientific, UK). The drug content was then calculated using a previously prepared calibration curve of the KAZ3 in acetone. The encapsulation efficiency was determined using the following equation:

$$EE\% = \frac{Actual amount of active present informulation}{the oritical amount of active} X100 \tag{1}$$

The KAZ3 release experiments were carried out in a shaking water bath (stuart SBS40, UK) at 37° C and 60 rpm. Briefly, 1 mg of each formulation was suspended into 2 mL PBS (pH = 7) in microcentrifuge tubes. The whole experiment was performed under sink conditions. At definite time interval, the formulations were centrifuged, and 1.5 mL of the sample were aspirated and were replaced with freshly prepared PBS. The absorbance of each sample was measured at λ_{max} of 350 nm. Both experiments were conducted in triplicates and average data were calculated.

2.10. siRNA polyplexes formation and N/P ratios determination using agarose gel electrophoresis

MDR-1 siRNA (277 ng) was mixed with varying amounts (0.14—4.72 μ g) of PEI-PL coated MSNs, 2.5 KDa coated PEI MSNs or 25 kDa coated PEI MSNs in nuclease free water to obtain N/P ratios of 0.5–100. The mixtures were vortexed for 5 s and incubated at room temperature for 10 min to allow polyplexes formation. Predesigned Silencer select MDR-1 siRNA has 21 base pairs, so each molecule of

siRNA contains 42 negative phosphate groups. N/P ratio was calculated using the following equation

$$\frac{N}{P} = \frac{number of moles of PEIxn^*}{number of moles of siRNAx42}$$
 (2)

where n is the amount of nitrogen in each PEI mole and equal to 57 in PEI 2.5KD and 580 in PEI 2.5KD.

An agarose gel electrophoresis was carried out to determine the siRNA conjugation to different coated MSNs. 1 μL of 10 x blue juice loading buffer was added to 9 μL of the formed polyplex and electrophoresed in 4 % agarose gel containing SYBRTM Safe as a gel Stain and 0.5 X TBE was used as the running buffer. The gel electrophoresis process was conducted at ambient temperature and at applied voltage of 55 kV for 30 mins. Stained siRNA bands were visualised by UV light and the images were captured using a Gel DocTM EZ gel imaging system (bio-rad, UK).

2.11. siRNA encapsulation efficiency and release (desorption)

A spectrophotometric analysis was used to determine the amount of siRNA that bound in the polyplexes at different N/P ratios. A volume of 40 μL of polyplexes was prepared according to the previously mentioned procedure. The formed polyplexes were then centrifuged at 13500 rpm at 4° C for 10 min and the supernatant was then aspirated. The unbound siRNA content in the supernatant was determined using NanoDrop spectrophotometer (Thermo scientific, UK) at a wavelength of 260 nm. The siRNA loading efficiency was easily calculated using the following equation:

$$\textit{EE\%} = \frac{\textit{TotalamountofaddedsiRNA} - \textit{amountofunboundsiRNA}}{\textit{TotalamountofaddedsiRNA}} \textit{X} 100 \qquad (3)$$

To study siRNA release from polyplexes, the supernatant was replaced with 40 μL PBS buffer (pH =7.4). The polyplexes were maintained at 37° C and was shacked at 60 rpm. The polyplexes were centrifuged at predetermined time intervals, and the cumulative siRNA amount was measured in the supernatant at a wavelength of 260 nm. The polyplexes were vortexed after each analysis.

2.12. ζ-potential measurement of nanoparticles/siRNA polyplexes

Subsequently, ζ -potential studies of the previously formed polyplexes at different N/p ratios were performed. The polyplexes could form for 10 min at room temperature and 1 mL of PBS was added to each sample.

2.13. Cell culture

Human colorectal cancer cell lines (HCT 116) were routinely cultured in a Modified McCoy's 5A medium supplemented with 10 % FBS in a cell culture incubator at 95 % humidified atmosphere and 5 % CO2 at 37° C. The growth medium was renewed every 2–3 days and the cells were passaged after trypsinization when they reach to 80 % cell confluency. In this study, HCT 116 were used at passages of 5–10.

2.14. Cellular uptake

HCT 116 cells were seeded on six-well plates at a seeding density of 3 X 10^5 cells per well and were cultured for 24 hrs to allow cell adherence. Drug loaded formulations (equivalent to 1 ug/ml KAZ3) were conjugated with Cy3-labeled siRNA to evaluate their uptake efficiency. The cells were incubated with the conjugates for 1 h and 24 h. After incubation time, the cells were washed with PBS three times and then were imaged using fluorescence microscope (InvitrogenTM EVOS, UK).

2.15. Cellular viability assay

MTT assay was used to determine the cytotoxicity of different KAZ3 loaded formulations and assessing the potential toxicity of empty coated MSNs.

The HCT-116 were cultured in 96 well plate at a seeding density of 10,000 cells per well for 24 h to allow the cells to attach before the experiment. The cells were then incubated with a fresh media containing different concentrations of free KAZ3, KAZ3 loaded MSNs (uncoated), KAZ3 loaded PEI-PL coated MSNs, KAZ3/siRNA loaded PEI-PL coated MSNs, empty PEI-PL-MSNs and empty 25 k PEI -MSNs for 48 h. After incubation time, the media containing samples were replaced with 100 μL of media containing 0.5 mg/mL MTT reagent. The plate was then incubated at 37° C for 1hr. The media was aspirated and 100 μL of DMSO was added to dissolve the formed formazan crystals. The absorbance of the coloured formazan solution was then measured at 590 nm using microplate reader (Generic 96 Promega Glomax Discover). The percent cell viability was calculated using the following equation:

$$\% cell \ viability = \frac{absorbance \ of \ treated \ cells - absorbance \ of \ blank}{absorbance \ of \ control \ cells - absorbance \ of \ blank} \ X10$$

$$\tag{4}$$

 * where blank was 100 μ L of 0.5 mg/mL MTT in media and control were the absorbance of untreated cells after MTT reagent application.

All measurements were done in triplicate and both average and standard deviation were calculated. IC50 (concentration of cytotoxic agent required to kill 50 % of cancer cells) of KAZ3 and different formulations were also calculated.

2.16. Western blots

HCT 116 cells were seeded in 25 cm² flasks at a seeding density of 1 X 10^6 cells per flask in 5 mL media. The cells were incubated for 24 hrs to allow to attach. The media was aspirated and then 5 mL of fresh medium (serum free) containing siRNA polyplexes of different formulations (at different N/P ratios) was added individually to each flask. The concentration of siRNA was kept 5 nM for all formulations to ensure maximum potency and the siRNA transfection was allowed for 48 hrs. The cells were then washed with ice-cold PBS buffer and were lysed in chilled RIPA buffer containing 0.1 mg/mL DTT. The obtained lysates were sonicated for 10 s and were centrifuged at 4 °C for 12 min at 15,000g. The Bio-Rad DC Protein Assay kit was used to determine protein concentrations in lysates.

Cell lysates containing 50 μg proteins were denatured using SDS sample buffer at 42 $^{\circ}C$ for 15 min and then were electrophoresed on a 7.5 % pre-casted polyacrylamide SDS gel at 120 kV for 1 hr. After

proteins separation, proteins were electro-transferred to 0.45 μm nitrocellulose membrane at 4 $^{\circ}C$ and at applied voltage of 70 kV for 90 min. The membranes were then blocked in 4 % non-fat milk in Trisbuffered saline containing 0.05 % Tween 20 (TBST) for 1 hr at ambient temperature. The blocked membranes were washed three times with TBST and were then incubated with primary antibodies; rabbit anti-human MDR-1 antibody and rabbit anti-human β -actin antibody. Herein, β -actin was used as a house keeping gene to monitor the loading accuracy. After three washes with TBST, membranes were incubated with goat anti-rabbit HRP-linked secondary antibodies at room temperature for 1 h.

Following additional three washes with TBST, 5 mL ECL substrate was added to each membrane and after 1 min, membranes were imaged using a UV illuminator (Biorad, UK).

3. Results and discussion

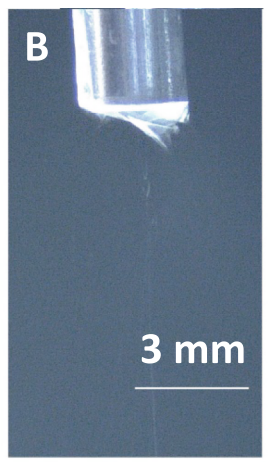
3.1. Jetting modes

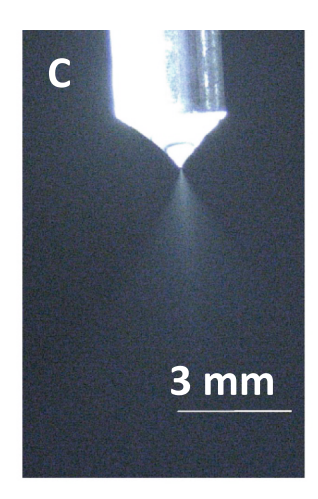
Fig. 1 displays different four Jetting modes at the orifice of the needle during electrospraying. Fig. 1 A shows the dripping mode (no jet) when a low insufficient voltage was applied to the electrospraying liquid. By further increase in the voltage the unstable jetting mode occurred (Fig. 1 B). Fig. 1 C displays the stable single jet mode and the formation of a Taylor cone. This is accomplished when the relation between flow rate and voltage were favourable. With further increase in the voltage a stable multi-jet was achieved (Fig. 1 D). The particles can be collected either in the single jet mode or multi-jet mode.

3.2. Particle composition

The previous study proved the ability of electrospraying method to load KAZ3 inside the mesopores of different types of mesoporous silica particles in an amorphous state [9]. The aim of the present study is to investigate, for the first time, the ability of electrospraying to coat MSNs with PL-PEI composite while KAZ3 loading process, simultaneously. Therefore, different formulations were prepared including, uncoated MSNs (K-MSNs), MSNs coated with 1:1 PLs and 2.5 K PEI (single needle coated formulations (MSNs- PEI-DOPE-SN, MSNs- PEI-PC-SN) and coaxially coated formulations (MSNs- PEI-DOPE-CO, MSNs- PEI-PC-CO, MSNs-PEI-PC-CO), MSNs coated with 2.5 K PEI only (MSNs-PEI-CO) and MSNs coated with 25 K PEI (MSNs-25kPEI-CO). The different composition of each formulation and their encapsulation efficiencies are listed in Table 1.







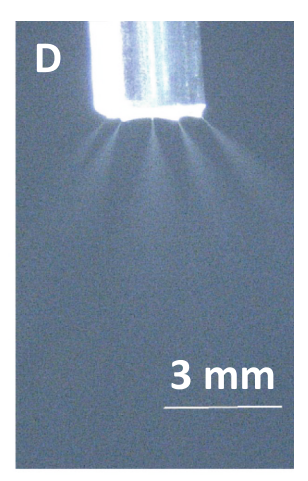


Fig. 1. Jetting images A) micro-dripping B) unstable jetting C) stable cone jet D) stable multi-jet.

3.3. Microscopic imaging (SEM and fluorescence microscopy)

The SEM and fluorescence microscopy images are demonstrated in Fig. 2 A and B, respectively. The fluorescence microscopy was used to assess the core–shell structure of KAZ3 loaded coated MSNs before and after Cy3-siRNA binding. It was found that using coaxial electrospraying technique, KAZ3 was uniformly dispersed inside the mesoporous matrix

of MSNs (Fig. 2B ii), after Cy3-siRNA binding, a red layer was noticed around the particles indicating the binding of siRNA to the PEI molecules that is surrounding MSNs. On the other hand, MSNs coated using single needle electrospraying technique was shown to have their KAZ3 content outside the mesoporous matrix and was preferably found surrounding MSNs (Fig. 2B vi). This could be related to the hydrophobic nature of KAZ3 thus KAZ3 was attracted to the lipid containing coating

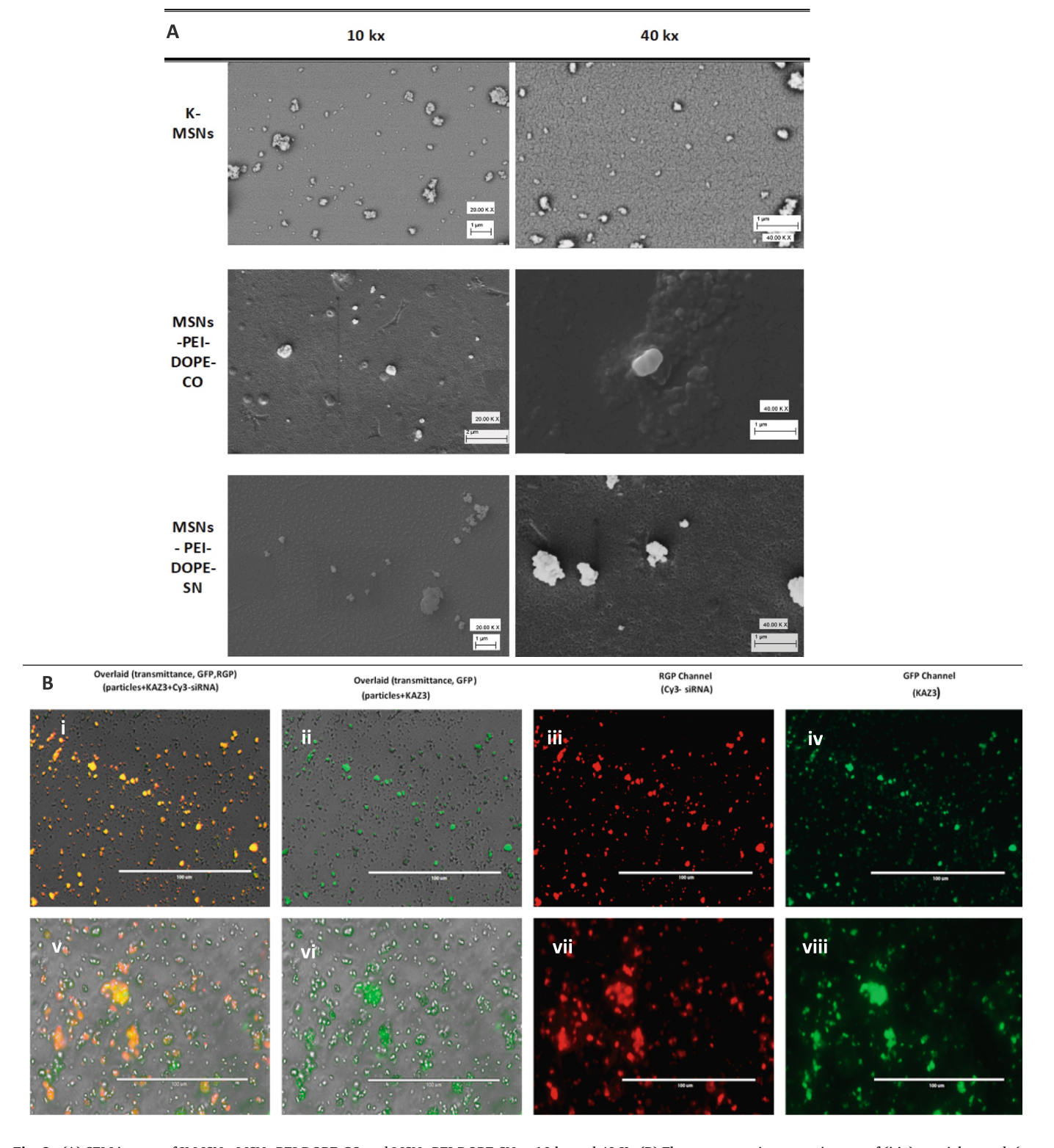


Fig. 2. (A) SEM images of K-MSNs, MSNs-PEI-DOPE-CO and MSNs-PEI-DOPE-SN at 10 kx and 40 Kx (B) Fluorescence microscope images of (i-iv) coaxial coated, (v-viii) single needle coated formulations before and after Cy3-siRNA binding at different channels (scale bar 100 μm).

layer more than the hydrophilic silica core. KAZ3 behaviour is attributed to the presence of KAZ3 molecules with the coating solution (PEI-PC) in the same needle during single needle electrospraying. In contrast, coaxial electrospraying provided two different needles; an inner needle for core materials (MSNs and KAZ3) and an outer needle for the shell materials (PEI and PL).

3.4. Physicochemical characterization of differently coated formulations

The different formulations before siRNA conjugation (including coated and uncoated MSNs) were characterized by means of TGA, DSC, XRD contact angle FTIR, particles size and ζ -potential measurements.

3.4.1. Thermogravimetric analysis studies

TGA analysis was used to assess the PEI-PL content in each unloaded coated formulation. The thermograms of MSNs before and after PEI-PL coating is demonstrated in Fig. 3A. The PEI-PL percent in each formulation was calculated after correcting TGA thermograms from water content by subtracting the weight loss of MSNs from the weight loss of each formulation at the temperature range $100-500\,^{\circ}$ C. Weight loss was calculated at $500\,^{\circ}$ C, as by this temperature all PEI and PL content had completely degraded. The calculated PEI content are shown in Table 2. PEI content in coated formulations varied from $16\,^{\circ}$ 6 to $25\,^{\circ}$ 6. These results indicates that EHDA was successful in grafting PEI on MSNs. The calculated PEI content in each formulation was used in determining the N/P ratio.

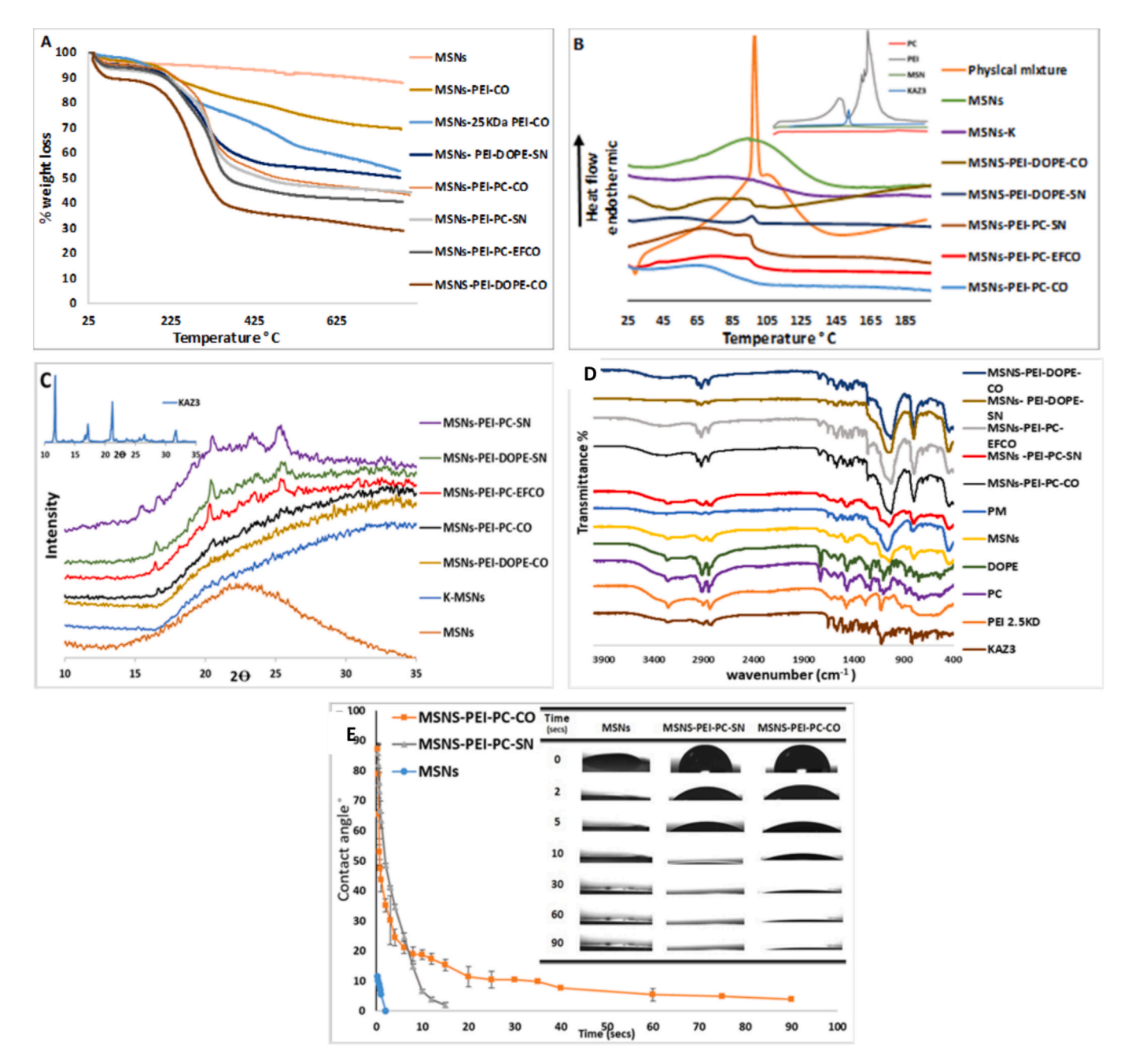


Fig. 3. (A) TGA, (B) DSC, (C) XRD, (D) FTIR and (E) Contact angle (the inset: digital images of water droplets on each formulation surface captured at different time intervals) of different coated formulations and pristine materials. SN: single needle electrospraying, CO: outer needle double flow rate coaxial electrospraying and EFCO: equal flow rate coaxial electrospraying.

Table 2 PEI content as calculated from TGA, particle size and ζ - potential values of different formulations

Formulation	TGA wt. loss (%) (100–500 °C)	PEI content % w/w	Particle size	ζ- potential
MSNs	5.1	0	30.7 \pm	–33.2 \pm
			3.3	7.2
MSNs -PEI-PC-	48.7	22	58.6 \pm	10.0 \pm
SN			9.4	0.4
MSNs- PEI-	37.2	16.1	35.9 \pm	13.5 \pm
DOPE-SN			1.0	4.5
MSNs-PEI-PC-	48	21.5	37.8 \pm	$21.6\pm0.$
CO			0.4	8
MSNS-PEI-	56	25	48.6 \pm	21.9 \pm
DOPE-CO			1.4	1.4
MSNs-PEI-CO	23.1	18.1	70.7 \pm	21.8 \pm
			11.7	3.9
MSNs-25KDa	30.4	25.4	90.0 \pm	40.4 \pm
PEI-CO			2.3	1.6
MSNs-PEI-PC-	53.6	22.4	48.3 \pm	15.5 \pm
EFCO			4.0	2.3

3.4.2. Size and ζ -potential studies

The particle size and ζ -potential of different formulations are listed in Table 2. The results illustrate that the uncoated MSNs were uniform in particle size and were smaller than the coated formulations. The average particle size of uncoated MSNs was 30 nm, while for electrosprayed coated formulations (e.g., MSNs-PEI-DOPE-SN and MSNs-PEI-DOPE-CO), the average particle size was 35 and 48 nm, respectively.

 ζ - potential of different coated formulations was measured (Table 2) and was used to evaluate the presence of the coating materials. The ability of coated MSNs to condense siRNA within PL-PEI coated MSNs is essential for successful gene delivery. In this sense, the coated MSNs are expected to have enough positive charge to complex the negatively charged siRNA molecules and lead to formation of polyplexes. The uncoated MSNs exhibited a negative charge of -33.2 mV because of the presence of negatively charged free surface silanol groups. However, all coated formulations showed a positive ζ -potential owing to the presence of positively charged PEI molecules. It was noticed that the ζ -potential values of coaxially coated MSNs were higher than single needle ones.

For example, ζ -potential value of MSNs-PEI-PC-CO was 21.6 mV, while that of MSNs-PEI-PC-SN was 10 mV. This indicates that a better coating was achieved using coaxial electrospraying technique than single needle electrospraying.

For coaxial electrospraying, infusing the external shell solution in a double rate (50 $\mu L/min)$ of the internal core solution (25 $\mu L/min)$, e.g MSNs-PEI-PC-CO, resulted in a higher ζ -potential than the electrosprayed formulations that used equal flow rates in both needles (MSNs-PEI-PC-EFCO). This suggests an enhanced coating was achieved when using a double flow rate in the external solution during coaxial electrospraying.

MSNs coated with 25 KDa PEI exhibited remarkably high ζ -potential when compared to formulations coated using 2.5 KDa PEI. The mean ζ -potential of MSNs coated with 25 KDa PEI (MSNs-25 KD PEI-CO) was 40.39 mV, whereas the mean ζ - potential of MSNs coated with 2.5 KD PEI (e.g., MSNs-PEI-CO) was 21.79 mV.

Combining PL (PC or DOPE) in the coating layer with 2.5 KDa PEI did not affect the overall ζ - potential of the electrosprayed formulations when compared to formulations coated with 2.5 KDa PEI only. For example, MSNs-PEI-PC-CO, MSNs-PEI-DOPE-CO and MSNs-PEI-CO exhibited ζ -potential of 21.55, 21. 93 and 21.79 mV, respectively. This is attributed to the fact that these PL molecules are neutral, and these formulations have approximately similar content of PEI (Table 2).

3.4.3. DSC and XRD studies

DSC and XRD charts of drug loaded formulations are shown in Fig. 3 B and C, respectively. The thermograms of pure KAZ3 and the physical mixture of MSNs and KAZ3 show a sharp endothermic peak at $101~^{\circ}$ C

indicating a high crystallinity of the drug [9,49]. The XRD chart of the pure KAZ3 shows multiple diffraction peaks confirming the high crystallinity of the drug. Loading of KAZ3 inside uncoated MSNs using electrospraying (K-MSNs) resulted in disappearance of the drug endothermic peak in its thermogram (Fig. 3 B) and in absence of any diffraction peak in its XRD pattern. These two findings indicate that electrospraying of KAZ3 with MSNs has successfully entrapped the drug molecules inside silica mesopores in its amorphous state, this outcome is consistent with our previous study [9]. DSC and XRD were also used to evaluate the effect of the electrospraying technique (single needle or coaxial) used for coating and loading KAZ3 into MSNs as an amorphous state. The DSC thermograms (Fig. 3 B) of the coaxial electrosprayed formulations (i.e. MSNs-PEI-PC-CO and MSNs-PEI-DOPE-CO) show no endothermic peaks indicating a complete entrapment of KAZ3 in the mesopores of MSNs in its amorphous state [50-52]. In contrast, the thermograms of single needle coated formulations (i.e. MSNs-PEI-PC-SN and MSNs-PEI-DOPE-SN) exhibit a sharp endothermic peak at 101 °C but with lesser magnitude than the original melting peak of KAZ3 which indicates that only some of the drug was loaded into the mesoporous silica pores but the rest was left outside the pores mixed with the coating materials in its crystalline state.

The XRD data (Fig. 3 C) is in a good agreement with the results obtained from DSC studies. There are no diffraction peaks noticed in the XRD patterns of the coaxially coated formulations (i.e. MSNs-PEI-PC-CO and MSNs-PEI-DOPE-CO). This indicates a complete amorphization of the drug has been fulfilled using this method. This further suggests that KAZ3 is completely loaded inside MSNs mesopores. On the other hand, single needle coated formulations (i.e. MSNs-PEI-PC-SN and MSNs-PEI-DOPE-SN) shows multiple diffraction peaks (at 17° , 21° and 26°) that are similar in pattern to those present in the crystalline drug (inset in Fig. 3 C). This assumes the presence of a considerable amount of crystalline unloaded drug within these formulations.

The XRD and DSC data suggest that coating of MSNs using coaxial electrospraying did not interpose with the ability of electrospraying to load MSNs with KAZ3 in one step. This might be attributed to the fact that this technique uses two individual needles for each liquid (i.e. internal for MSNs/ KAZ3 suspension and external for Pl-PEI coating material) which minimized the interaction between the two process. In contrast, using single needle electrospraying technique to coat MSNs did not successfully work to load the drug within MSNs in the same process. As most of the drug was entrapped in the coating materials (PL and PEI) surrounding MSNs. This is clearly supported by the fluorescence microscope image (Fig. 2 B vi).

3.4.4. FTIR studies

The FTIR spectra of different pristine materials and coated formulations are presented in Fig. 3 D. Compared to MSNs spectrum, the FTIR spectra of coated formulation presented new peaks corresponding to PL and PEI structure. Spectra of all coated formulations display transmittance bands at $\sim 1250~\rm cm\textsc{-}1$ and 1735 cm-1 related to asymmetric stretching vibration of P=O in phosphate group and to C=O stretching of ester carbonyl groups, respectively. The presence of P=O and C=O bands is only attributed to PL structure rather than silica structure, suggests that the PL was successfully grafted on MSNs. The wide transmittance band at 3271 cm-1 is related to the stretching vibration of O-H of silanol group and this peak is further corresponding to N-H group of PEI in coated formulations.

3.4.5. Contact angle studies

As presented in Fig. 3 E, the water droplet on the pristine MSNs surface exhibited a very low contact angle value (11.5°) and it spread instantly all over the surface of MSNs within 2 secs giving 0° contact angle. This behaviour is attributed to the superhydrophilicity of silanol groups which are abundant in mesoporous silica matrix and can bind with water molecules through hydrogen bonding. The quick spreading of water droplet is additionally due to the capillary condensation of

water through nanopores of MSNs [53,54]. Coating of MSNs with composite PEI-PL (e.g. MSNS-PEI-PC-SN, MSNS-PEI-PC-CO) has prominently increased the value of contact angle to 85.7° and 87.2°, respectively. This can be explained by the presence of the PL containing coating layer that is covering silica hydrophilic surface, therefore minimizing both wicking effect and hydrogen bonding with water. However, the value of contact angle of these was reduced over time differently.

For instance, the contact angle of MSNS-PEI-PC-CO was 87.1° initially and reached to value of 3.9° over 90 s. However, MSNS-PEI-PC-SN was 85.7° and attained its smallest magnitude 1.9° within 15 sec only. This reflects the time was taken for water molecules to penetrate through the coating layer to reach to silica mesopores. It is observed that the contact angle of MSNS-PEI-PC-CO took a longer time to decrease than that of MSNS-PEI-PC-SN (Fig. 3 E), is due a better coating was achieved using coaxial electrospraying than single needle electrospraying.

3.5. Encapsulation efficiency and in vitro release profile

The uncoated formulation (K-MSNs) showed a high EE% of 91.3 %. This result is consistent with the previous study results, where electrospraying was successful in loading KAZ3 in mesoporous silica particles with a high EE%. Using coaxial and single needle electrospraying methods for coating MSNs with PL and PEI have achieved similar EE% to the uncoated MSNs. For example, MSNs- PEI-DOPE-SN and MSNs-PEI-DOPE-CO have attained high EE% of 94.6 % and 90.8 %, respectively.

The release patterns of KAZ3 from pure drug crystals, drug loaded uncoated MSNs and coated formulations are presented in Fig. 4. The release profiles of formulations showed bi-phasic release patten; an initial fast burst phase followed by steady state phase. The release rate of KAZ3 from electrosprayed uncoated drug loaded MSNs (K-MSNs) was obviously greater than that of pure KAZ3, reaching a total of 70 % from K-MSNs when compared to only 2.49 % drug from drug crystals and of after 48 h. This greater enhancement of drug dissolution rate (28-folds) when using EHDA as a drug loading technique is due to its ability to achieve complete fitting of the drug within mesoporous matrix of MSNs in an amorphous state. This result is in a good agreement with our previous study that showed the ability EHDA as a loading technique for mesoporous silica to improve the solubility of poorly water-soluble

drugs [9].

Coating of MSNs with PEI-PL composite caused reduction in the burst release and produced more sustained release profile. For example, K-MSNs showed a fast burst release for the first 6 hrs (57.7 %), which is much higher than that of MSNs-PEI-PC-CO (48.9 %) and of MSNs-PEI-DOPE-CO (37.1 %). After 48 h., 70 % of KAZ3 was released from uncoated MSNs loaded nanocarrier (K-MSNs) while, coated MSNs based nanocarrier (e.g. MSNs-PEI-DOPE-CO and MSNs-PEI-PC-CO) released 48.4 % and 64.3 % of their content, respectively. This might be attributed to the presence of a composite PL and PEI layer on top of MSNs surface which delayed the release of KAZ3 and resulted in more sustained release profile. This behaviour was previously noticed in other studies investigating coated MSNs [55,56].

Clearly, the amount of KAZ3 released from MSNs-PEI-PC-CO (64.3 %) is remarkably greater than that released from MSNs-PEI-DOPE-CO (48.6 %), indicating that the type of PL in the coating layer has a great effect on the release of the cargo and on achieving sustained release profile. The same notice was found when comparing MSNs-PEI-PC-SN, which released 43.2 % of its content, and MSNs-PEI-DOPE-SN that released only 26 %, by the end of the experiment. The results indicate that formulations with coating layer comprising PC showed a more enhanced dissolution rate than those comprising of DOPE. This can be explained by the different hydration properties of phosphatidylcholine and phosphatidylethanolamine groups. Studies found that PC dispersions in water can adsorb considerably more water molecules than DOPE. As the tight packed structure of DOPE reduces the permeation of water through its bilayers [57,58]. This suggests that water molecules can easily access the mesoporous matrix containing KAZ3 in the formulation coated with PC inducing the drug diffusion outside of the matrix. However, the permeation of water through DOPE coated MSNs was lower causing decreased diffusion of the drug from mesopores giving a poor dissolution profile. These different release patterns that could be achieved by controlling the coating layer could be a pathway for this drug delivery system in different biopharmaceutical applications.

Additionally, the method of electrospraying used for coating showed a considerable effect on the release of the drug. Obviously, the dissolution rate of coaxially atomized coated formulations was considerably higher than single needle atomized formulations. For example, after 6 h., MSNs-PEI-DOPE-CO and MSNs-PEI-PC-CO reached a total 37.1 %

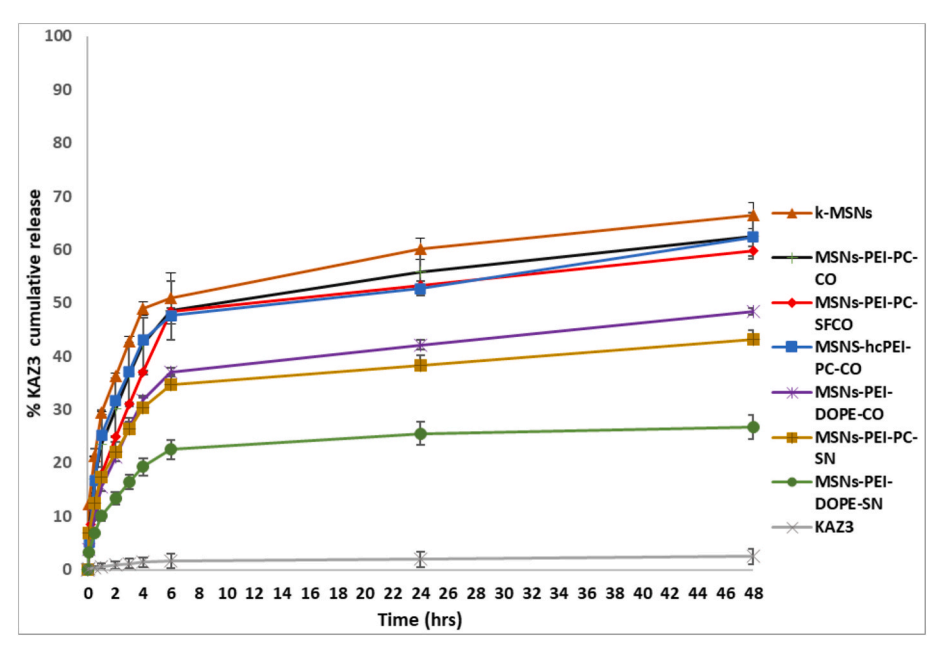


Fig. 4. In vitro release studies of KAZ3 from different formulations.

and 57.7 % of KAZ3 release, respectively. On the other hand, single needle coated MSNs (MSNs-PEI-DOPE-SN, MSNs-PEI-PC-SN) only attained a total of 22.5 % to 34.6 % KAZ3 release within the same time period. After 48 h, coaxially atomized formulations achieved between 48.4 and 64.3 % of their KAZ3content, whereas formulations coated using single needle electrospraying released 26 to 43.2 of its contents. This can be explained by the presence of KAZ3 within mesopores of the coaxial coated formulation as complete amorphous form, while a great amount of crystalline unloaded drug is present within single needle formulations as supported with XRD data (Fig. 3 C).

3.6. Characterization of differently coated formulations as siRNA delivery vehicles

3.6.1. Gel retardation study

PEI is a polycationic polymer that can electrostatically interact with nucleic acid including siRNA [24]. It is common that the ability of PEI to complex siRNA decreases when the backbone of PEI is conjugated with PL [27]. Therefore, assessing the ability of the prepared particles to condense siRNA is an essential step in characterization of the novel coated particle. As discussed earlier in section 4.1, the PEI transfection capability is greatly affected by N/P ratio thus, siRNA binding ability of formulations was tested at different N/P ratios.

At the beginning, a wide range of N/P ratios (3–100) was examined. As shown in Fig. 5 A, all coated MSNs were found to be effective to retard siRNA at each N/P ratio of this range. Therefore, a smaller range of N/P ratios (0.5–6) was utilized. As demonstrated in Fig. 5 A, PEI conjugation with PL did not decrease the binding capacity of PEI. This result is consistent with the outcomes of other studies that examined the effect of PL conjugation with PEI [25,27].

The mobility of siRNA in all coated formulations was completely retarded at N/P ratio 3 or more (As shown in Fig. 5 A). It is clear that

coaxial needle coated formulations (i.e. MSNS-PEI-PC-CO and MSNS-PEI-DOPE-CO) demonstrated fainter siRNA band than single needle coated formulations (i.e MSNS-PEI-PC-SN and MSNS-PEI-DOPE-SN) at N/P ratio 0.5 and 1 indicates a better siRNA condensation for the coaxially coated formulations even at a very low N/P ratio. This result is accounted by the better coating that was accomplished by the coaxial electrospraying compared to single needle electrospraying. Additionally, as seen in the florescence microscopy images (Fig. 2 B), some of the drug crystals were entrapped in the coating material (PL-PEI) of the single needle coated formulations. The drug present in the coating material decreased the binding capacity of these formulations.

3.6.2. siRNA binding and encapsulation efficiency

The complexation ability of different coated formulations with siRNA was evaluated using UV spectrophotometric measurements (Nanodrop instrument). In this method, different amounts of coated MSNs were incubated with the same concentration of siRNA and then centrifuged to precipitate siRNA formed polyplexes. The concentration of the unbound siRNA in the supernatant was then measured at 260 nm. Fig. 5 B shows the encapsulation efficiency (percentages of bound siRNA) are presented as a function of N/P ratio in.

All formulations exhibited an siRNA EE % higher than 90 % at N/P ratio 16 or more regardless of coating method. In contrast, the coating method greatly affected the siRNA EE % at N/P ratios 6 or lower. It was found that single needle coated MSNs showed lower EE % than coaxially coated MSNs at N/P ratios 6 or lower (Fig. 5 B). For example, at N/P ratio 0.5 both single needle coated formulations (i.e MSNs-PEI-PC-SN and MSNs-PEI-DOPE-SN) showed EE % around 30 % while coaxially coated formulations (MSNs-PEI-PC-CO) and MSNs-PEI-DOPE-CO) showed EE % of 50 % approximately. Similarly, at N/P ratio 6 the siRNA EE% of single needle coated particles was lower (around 80 %) compared to that of coaxially coated particles (around 95 %). This

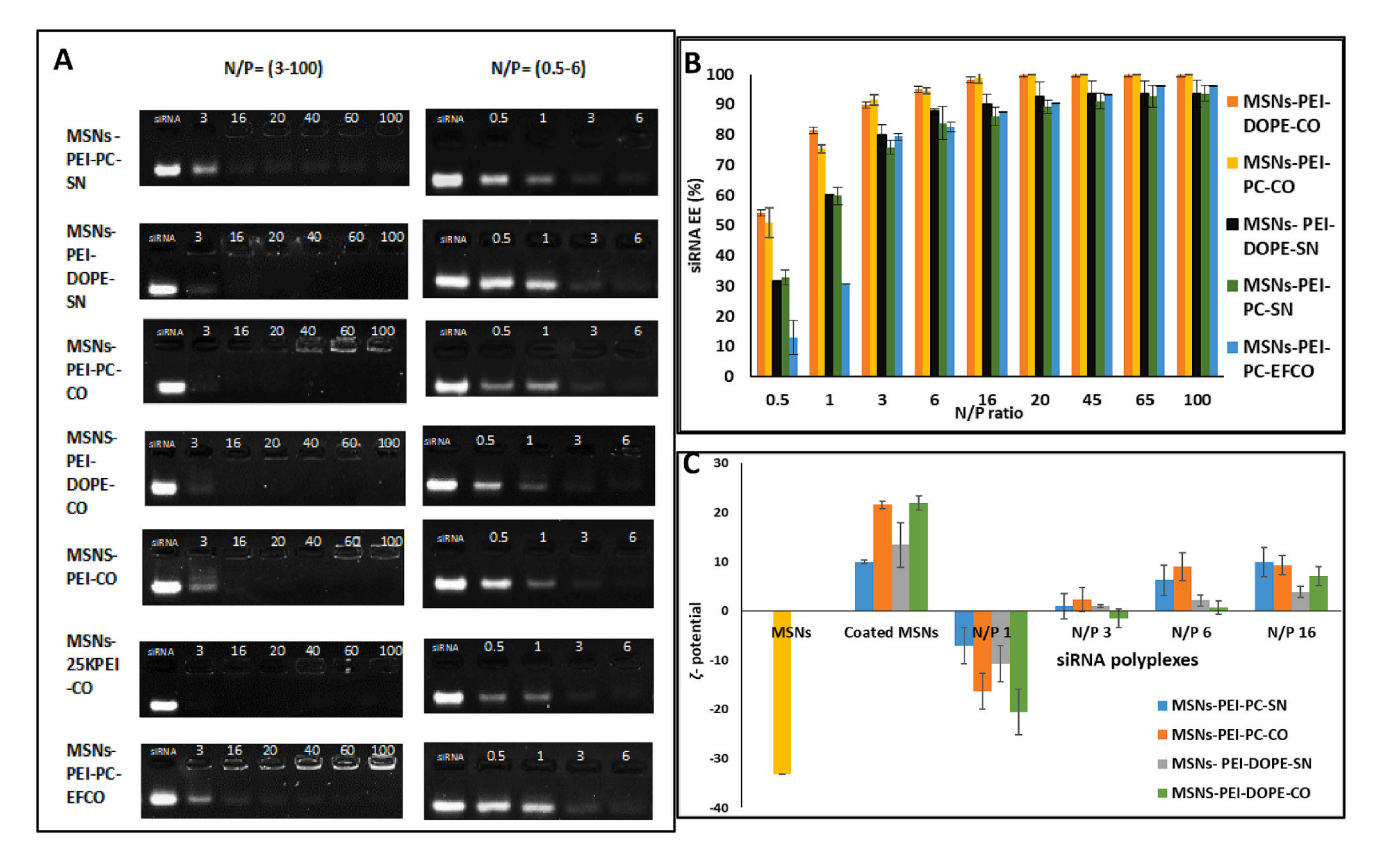


Fig. 5. (A) Agarose gel retardation (B) siRNA EE% of different electrosprayed MSNs at different N/P ratios and (C) ζ-potential values of MSNs and different PL-PEI coated MSNs before and after siRNA loading at different N/P ratios. SN: single needle electrospraying, CO: outer needle double flow rate coaxial electrospraying and EFCO: equal flow rate coaxial electrospraying.

indicates better complexation of siRNA with coaxially coated particles than single needle one. The composition of the coating material of did not change siRNA encapsulation. These results are consistent with the gel retardation study.

3.6.3. Polyplexes ζ-potential

To further characterize the formed siRNA polyplexes, their ζ -potential values were measured. As discussed before, PL-PEI coated MSNs are positively charged particles (approximately 10 mV to 21 mV, Table 2). After siRNA conjugation, ζ -potential values of the formed polyplexes generally became less positive or negative, depending on the N/P ratio and on the formulation type as demonstrated on Fig. 5 C. For example, at N/P ratio of 1, ζ -potential of all tested formulations was negative, reaching - 20.1 mV and -16.3 mv for MSNS-PEI-DOPE-CO and MSNS-PEI-PC-CO, respectively. Formulations with lower siRNA EE % (e.g. MSNS-PEI-DOPE-SN and MSNS-PEI-PC-SN) afforded higher ζ potential values of -10.6 mv and -7.1 mv, respectively. As shown in Fig. 5 C, it is clear that the value of ζ potential is increasing with increasing N/P ratio. As by increasing the N/P ratio, PEI content increases thus rendering more positive charges to the surface of polyplexes. For example, at N/P ratio 16 the ζ -potential of MSNS-PEI-DOPE-CO was + 7.05 and that of MSNS-PEI-DOPE-SN was 3.65.

3.7. siRNA desorption (release studies)

The siRNA desorption from the coated MSNs should be tested to characterize the reversibility of the electrostatic interaction between PEI-PL coated MSNs. It is crucial for siRNA to be released from the formed polyplexes under physiological conditions to achieve ultimate bioactivity and gene silencing. Fig. 6 demonstrates the release patterns of siRNA from polyplexes formed by different formulations at varied N/P ratios and varied coating material structure. The release of siRNA from

coated MSNs was highly dependent on N/P ratio as shown in Fig. 6 A and B. It was found that at low N/P ratio, formulations released siRNA faster but by increasing N/P ratio the release of siRNA became a more sustained pattern. For example, MSNs-PEI-DOPE-CO released more than 60 % of its siRNA content by 4 h. and 70 % by 24 h. However, increasing the N/P ratio to 16 the same formulation released only 28 % and 36 % of its siRNA content by 4 and 24 h, respectively. The same behaviour is noticed by other formulations such as MSNs-PEI-DOPE-SN (Fig. 6 B). The PEI content is increased by increasing the N/P ratio, thus a stronger interaction between the formulations and siRNA is expected decreasing the siRNA desorption. Thus, optimizing the N/P ratio during the transfection experiment is important to ensure both binding and then desorption of siRNA from nanoparticles.

The effect of coating material on siRNA desorption was also investigated. As shown in Fig. 6 C, no substantial difference between formulations coated with 2.5 KDa PEI and those coated with composite of PEI either type of PL. However, formulation coated with 25 KDa PEI (MSNs-25KDa PEI) showed lower siRNA release than formulations coated with 2.5 KDa PEI. For example, by 24 h, MSNs-25KDa PEI released 25 % of its siRNA content but MSNs-PEI-CO, MSNs-PEI-DOPE-CO and MSNs-PEI-PC-CO released 53 %, 57 % and 48 %, respectively.

3.8. Cellular uptake of PEI-PL coated MSNs/ siRNA polyplex

The cellular uptake of PEI-PL coated MSNs/ siRNA polyplexes after 1 h and 24 h of incubation was confirmed using a fluorescence microscope (Fig. 7). In this experiment, drug loaded formulations were conjugated with red fluorescent Cy3-labeled siRNA to track the cellular uptake of both siRNA and the green, fluorescent KAZ3. After 1 h the PL-PEI coated MSNs were observed to be endocytosed by cells (Fig. 7 A), thus suggesting that coated particles were effectively internalized by HCT 116 cells. However, uncoated K-MSNs the particles were not observed to be

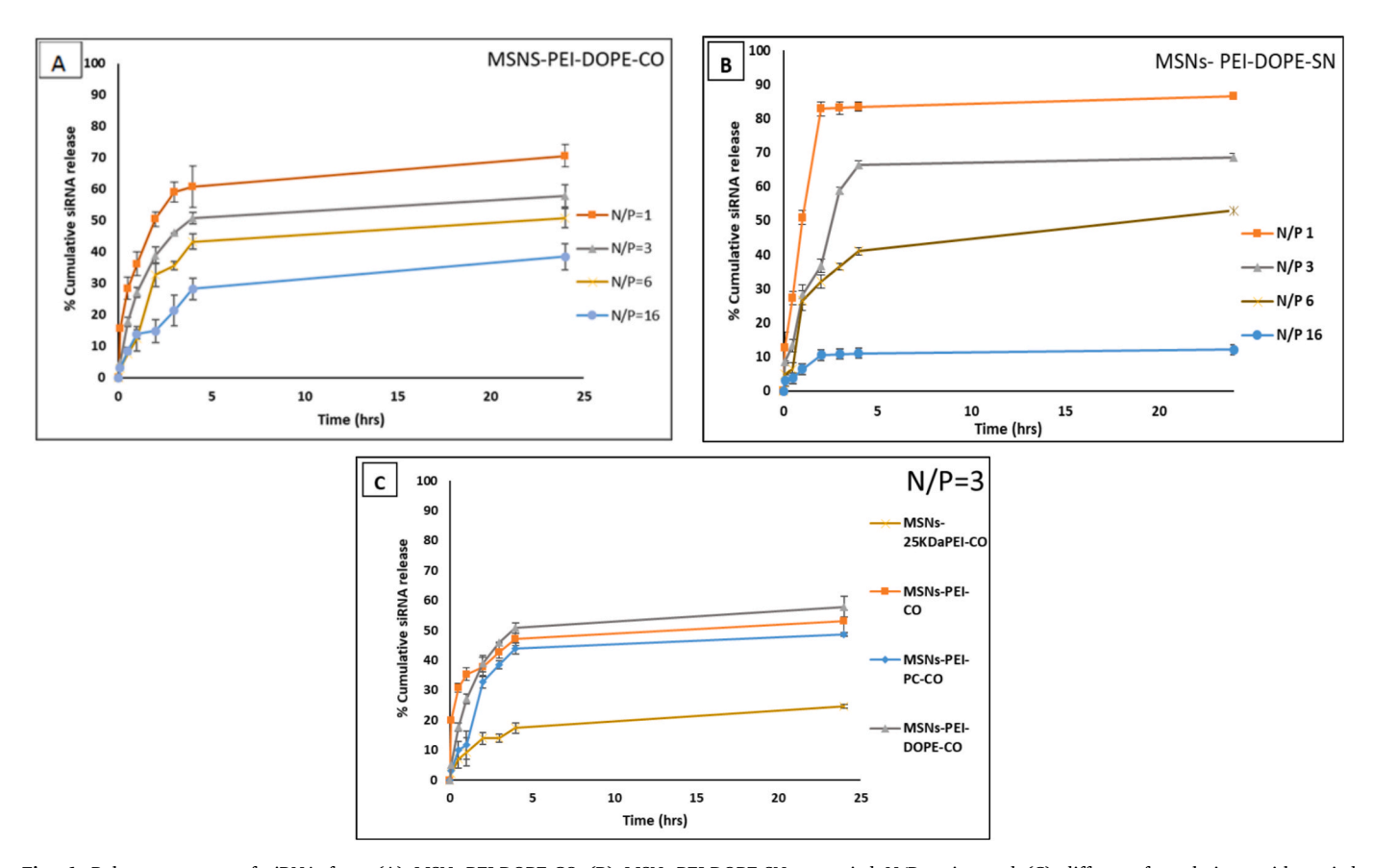


Fig. 6. Release patterns of siRNA from (A) MSNs-PEI-DOPE-CO (B) MSNs-PEI-DOPE-SN at varied N/P ratios and (C) different formulations with varied coating material.

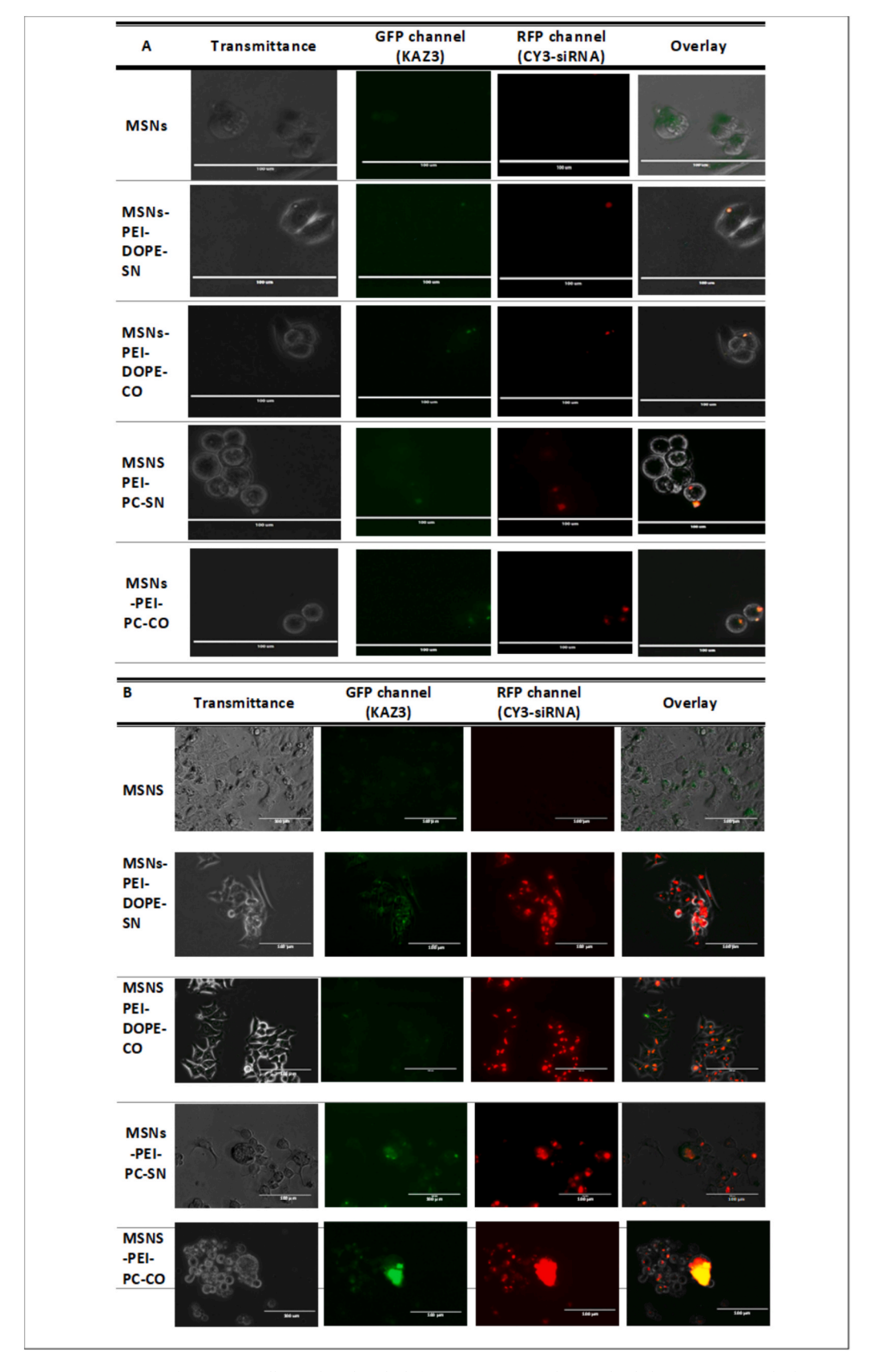


Fig. 7. Fluorescence microscope images of HCT 116 cells incubated with different PL-PEI coated KAZ3 loaded MSNs/siRNA polyplexes for (A) 1 h (B) 24 h at different microscope channels and after merging channels, (scale bar 100 μ m).

endocytosed but the released KAZ3 in the culture medium was internalized instead. This suggests that the presence of the coating layer of PEI and PL enhanced the cellular internalization of the particles themselves. At 24 h, the intensity of green and red fluorescence was increased significantly for all coated formulations as shown in Fig. 7 B. Also, the fluorescence (green or red) was not observed confined within the particles as seen on the images taken after 1 h (Fig. 7 A). This suggests that both siRNA and KAZ3 were successfully released from MSNs inside cells. This also shows that both actives were successfully escaped from the endosomes after endocytosis.

These results obviously suggest that PEI-PL coated MSNs are capable of penetrating into cancerous cells and simultaneously deliver KAZ3 and siRNA into the cellular cytoplasm, approving our theory that the novel PEI-PL coated MSNs can successfully co-deliver the cytotoxic drug and siRNA to the cancer cells.

3.9. Cytotoxicity studies

A principal consideration in the usage of PEI as a gene transfecting agent is its cytotoxicity. Therefore, it was essential to assess the cytotoxicity of MSNs coated with different MW PEI before assessing the cytotoxicity of KAZ3 loaded formulations in HCT 116. As shown in Fig. 8, MSNs coated with the 25 kDa PEI exhibited substantial cytotoxicity when the particle concentration was more than 5 μ g/mL (0.005 mg/ml). In contrast, MSNs coated with DOPE and 2.5 kDa PEI had no cytotoxic effects even at a particle concentration up to 100 μ g/mL (0.1 mg/ml). Therefore, PL-PEI coated MSNs is considered safe gene and drug delivery system. However, PL-PEI coated MSNs should be used at

concentration less than 100 μ g/mLin the delivery studies to avoid its cytotoxic effect. This finding also proves that PL-PEI coated MSNs are safer and less cytotoxic to human cells than 25 K PEI coated MSNs.

Moreover, it was observed that bare MSNs showed no cytotoxicity at all used concentrations, suggesting that MSNs are a compatible material with human cells even at high concentrations. Cytotoxicity of KAZ3 loaded formulations before siRNA conjugation was also assessed at different drug concentrations (0.6, 1, 2.5, 10 μg /mL) using MTT assay (Fig. 8 B). KAZ3 loaded MSNs (IC50 of 0.651 μg / mL) showed more cytotoxicity than pure KAZ3 (IC50 of 4.95 μg / mL) at all tested drug concentrations. For example, at 2.5 μg /mL drug concentration, pure KAZ3 caused 66 % cellular variability but KAZ3 loaded MSNs were more cytotoxic to the cells with only 20 % cell viability at the same concentration. This is attributed to improving the drug solubility and permeability achieved with the loading of the crystalline drug into the mesopores of MSNs. By loading the drug into the mesopores of MSNs the drug is transformed to its amorphous more soluble form.

The effect of coating on the performance of MSNs was also assessed. PC-PEI coating using coaxial electrospraying (MSNs-PEI-PC-CO) has an improved the cytotoxicity with only 14 % cell viability at the same concentration. This might be due to improvement of cellular uptake by PEI and PL coating [18]. However, MSNs-PEI-DOPE-CO showed lower cytotoxic effect than MSNs-PEI-PC-CO in all tested concentrations, this could be attributed to the lower KAZ3 dissolution of MSNs-PEI-DOPE-CO when compared to MSNs-PEI-PC-CO as shown in Fig. 4.

In contrast, formulations coated with single needle electrospraying demonstrated a lower cytotoxic effect. At 2.5 $\mu g/mL$ KAZ3 concentration, MSNs-PEI-DOPE-SN and MSNs-PEI-PC-SN caused 47 % and 25 %

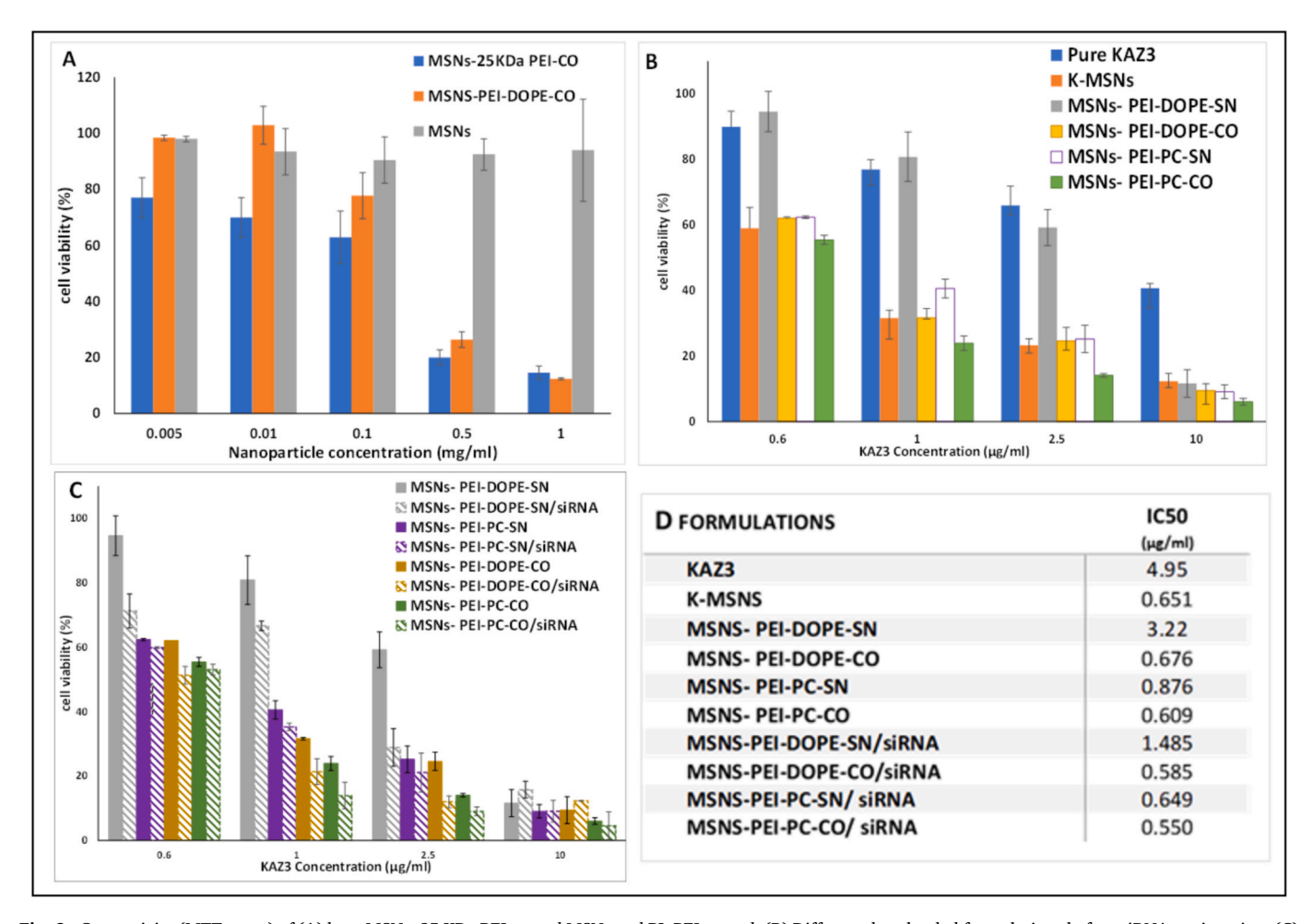


Fig. 8. Cytotoxicity (MTT assay) of (A) bare MSNs, 25 KDa PEI coated MSNs and PL-PEI coated, (B) Different drug loaded formulations before siRNA conjugation, (C) after siRNA conjugation at different drug concentrations as measured & (D) IC50 of pure KAZ3 and different drug loaded formulations.

cellular viability, respectively. The decrease in the cytotoxicity of single needle electrosprayed coated formulations than coaxially coated ones is associated with the partial crystallinity of KAZ3 within these formulations and their retarded KAZ3 dissolution as discussed before. Remarkably, the conjugation of MDR-1 siRNA to PEI-PL coated MSNs has further improved the cytotoxicity of all formulations and reduced their IC50 values as shown in (Fig. 8 B & D). For example, conjugation of siRNA with KAZ3 loaded MSNs-PEI-DOPE-CO (2.5 µg /mL KAZ3) improved the cytotoxicity of KAZ3 and resulted in 88.4 % cancer cell death while treating cells with KAZ3 loaded MSNs-PEI-DOPE-CO only at the same concentration caused 75 % cells death. Another example is MSNs-PEI-PC-CO (2.5 μg /mL KAZ3) which showed 86 % cytotoxicity and after siRNA conjugation it showed 92 % cytotoxicity. Moreover, these formulations (MSNs-PEI-DOPE-CO/siRNA and MSNs-PEI-PC-CO/ siRNA) showed the lowest IC50 (0.585 and 0.550 µg /mL, respectively) amongst all formulations.

Similar behaviour is observed with KAZ3 loaded MSNs-PEI-DOPE-SN (single needle coated formulation) which caused 41 % cancer cell death at 2.5 μg /mL and after siRNA conjugation caused 75 % cell death. These results clearly indicate that co-delivery of siRNA with KAZ3 loaded coated MSNs significantly inhibited HCT-116 cell growth. The great enhancement of KAZ3 anticancer effect with these formulations is attributed to improving its dissolution, enhancing its cellular uptake and silencing MDR-1 gene that is responsible for the resistance against anticancer drugs.

3.10. Western blotting (P-gp silencing)

The MDR-1 silencing efficiency mediated by PL-PEI coated MSNs/siRNA polyplexes was investigated using HCT-116. PL-PEI coated MSNs were tested at different N/P ratios in order to determine the best N/P ratio for a maximum knockdown efficiency. Image-J software was used

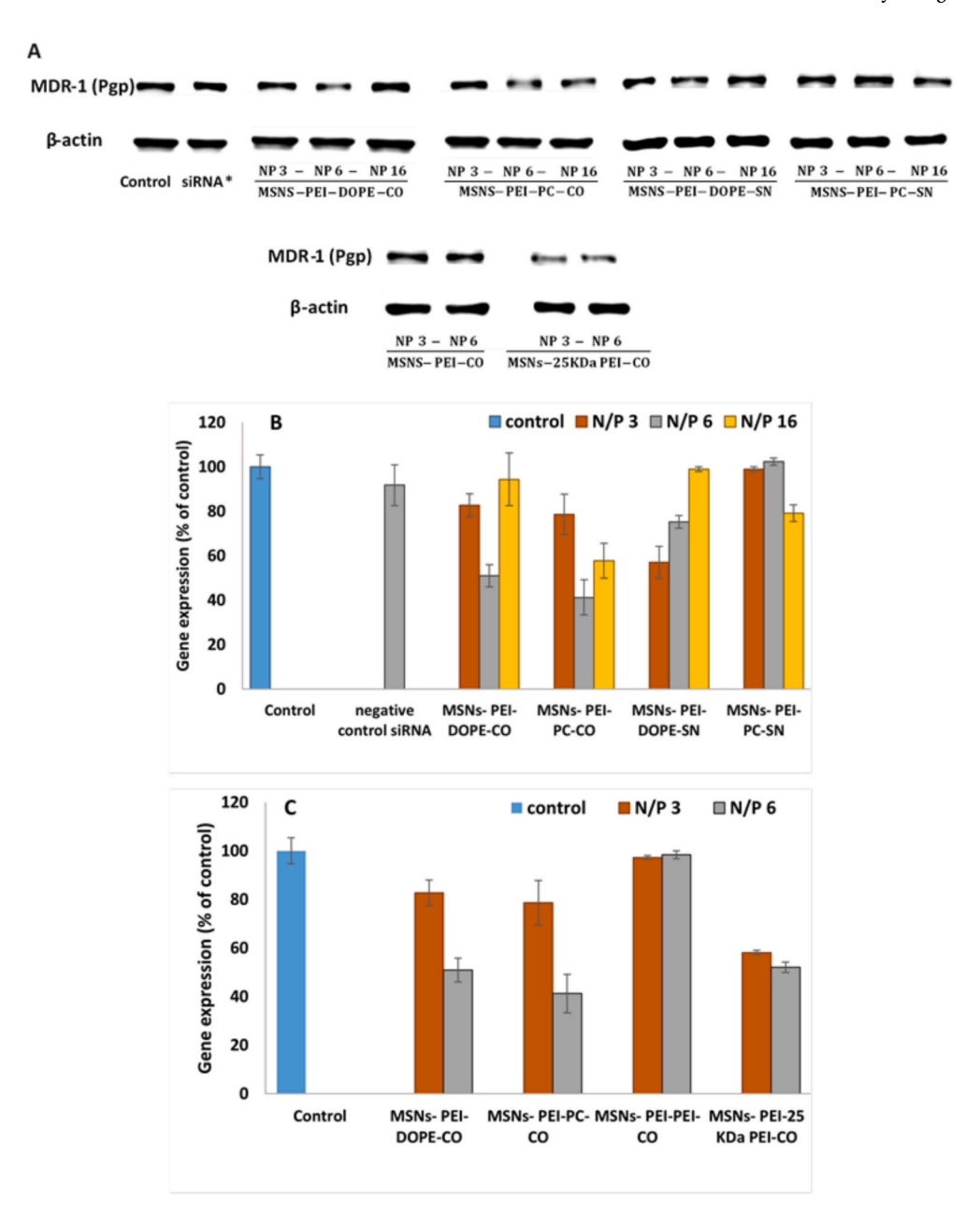


Fig. 9. (A) western blotting images detecting the target protein P-gp and the house keeping gene (β-actin). P-gp expression measured using image J software (B) effect of coating method on P-gp expression and (C) Effect of different N/P ratio and coating material on P-gp expression of HCT 116 after incubation with differently coated MSNs/siRNA polyplexes.

to calculate the P-gp expression from western blots graphs. The silencing of MDR-1 was measured by the decrease in the expression of the target Protein (P-gp) which was determined using western blot (Fig. 9 A).

Complexes based on MSNs coated with high MW PEI (25 KDa) caused approximately 50 % P-gp suppression. In contrast, no detectable P-gp gene knockdown was noticed with MSNs coated with unmodified low MW PEI (2.5 KDa) based-polyplexes as shown in Fig. 9 C. The lower transfection ability of low MW PEI is attributed to lower siRNA condensation and faster degradation rate [26,59]. The low transfection ability of low MW PEI is previously reported in several studies [25–28,59]. However, modification of PEI 2.5 KDa with PL effectively improved the gene silencing ability of coated MSNs. For example, DOPE modification (i.e MSNs-PEI-DOPE-CO) suppressed P-gp expression by 50 % while PC modification (i.e., MSNs-PEI-PC-CO) reduced the P-gp expression to 41 % at N/P ratio 6.

As displayed in Fig. 9 B, formulations coated with different electrospraying technique showed different silencing efficacy. It was shown that formulations coated with single needle electrospraying technique (e.g. MSNs-PEI-DOPE-SN and MSNs-PEI-PC-SN) showed lower gene silencing ability than coaxial coated formulations (e.g. MSNs-PEI-DOPE-CO and MSNs-PEI-PC-CO). For example, at N/P ratio 16, MSNs-PEI-DOPE-CO have achieved better gene silencing ability than MSNs-PEI-DOPE-SN as it lowered the expression of P-gp to 50 % compared to 75 % P-gp expression was achieved by MSNs-PEI-DOPE-SN. The same finding was noticed when comparing MSNs-PEI-PC-CO (41 % P-gp expression) vs MSNs-PEI-PC-SN (100 % P-gp expression) at the same N/P ratio.

It was demonstrated in Fig. 9 C, that N/P ratio highly affected the silencing efficiency of polyplexes. For example, at N/P ratio of 3 MSNs-PEI-PC-CO and MSNs-PEI-DOPE-CO based polyplexes caused only 22 %and 18 % P-gp suppression, respectively. By increasing the N/P ratio to 6, MSNs-PEI-PC-CO\ siRNA and MSNs-PEI-DOPE-CO\ siRNA were able to reduce the p-gp expression by almost 60 % and 50 %, respectively. This improvement in the gene silencing is attributed to increasing the positive charge by increasing N/P ratio. As shown in Fig. 5 C at N/P 3 siRNA polyplexes showed either negative or slightly positive (+2.3 MSNs-PEI-PC-CO) for but increasing the N/P to 6 increased the positive charges on the polyplexes to + 9 for MSNs-PEI-PC-CO. The overall positive charge of siRNA polyplexes is crucial for the electrostatic interaction with the negatively charged proteoglycans on the cellular membrane to promote the cellular uptake of polyplexes via endocytosis [25,28]. However, by increasing the N/P ratio to 16 the gene silencing ability of the polyplexes was reduced again. For example, and MSNs-PEI-DOPE-CO\ siRNA and caused only 7 % P-gp suppression. This reduction in the gene Knockdown ability at N/P ratio 16 is attributed to the reduced release of siRNA form the formed polyplexes as shown in Fig. 6.

It can be concluded that coaxial coated formulations demonstrated the best silencing efficiency Also, N/P ratio 6 was the best ratio to use in gene transfection experiment. Finally, PEI conjugation with PC PL demonstrated better silencing ability than DOPE PL.

4. Conclusion

Coaxial electrospraying has successfully coated MSNs with PL-PEI composite and loaded it with KAZ3, simultaneously in one single step. Thus, considered a time and effort efficient method. Coaxial electrospraying was efficient technique in loading MSNs with KAZ3 in a complete amorphous form when compared to using single needle electrospraying technique as a coating method as shown by the XRD results. It was also shown that coaxial atomized particles had an enhanced dissolution profile. Moreover, PL-PEI coated MSNs were found to conjugate to siRNA efficiently at very low N/P ratio. This study clearly demonstrated that MSNs coated with 2.5 K PEI and PL were compatible with human cells more than MSNs coated with high MW PEI. They were found safe non-toxic nanoparticle when used in concentration suitable for pharmaceutical applications. They were found to be effective to co-

deliver both KAZ3 and MDR-1 siRNA to cancer cell lines successfully.

Results indicate that MSNs coated with (1:1) PC and 2.5 K PEI demonstrated a high KAZ3 encapsulation efficiency of 89 % and an efficient siRNA binding capability with 93 % entrapment efficiency at N/P ratio 6. siRNA/ the optimal formulation was efficient as a gene transfecting agent as it caused up to 60 % MDR-1 gene silencing. KAZ3/siRNA loaded MSNs-PEI-PC-CO showed high cytotoxicity as it caused up to 92 % cancer cell death which is 3 folds the cytotoxicity of the pure drug at the same concentration. Therefore, this formulation allows the use of cytotoxic agents in lower doses thus the expected adverse effects of these drugs should be reduced. Moreover, its efficiency in gene silencing makes it a promising non-viral gene vector which can be used for treatment of other genetic based diseases.

In this research project we proved the concept of using EHDA to load and coat MSNs in a single-step technological advance. This research could be widened in the future by preparation of MSNs active targeting drug and environmentally responsive delivery systems should be explored. The ability of co-axial electrospraying to graft targeting ligand (e.g., galactose, folic acid and monoclonal antibodies) on mesoporous silica surface should be tested. Moreover, its ability to cap mesoporous silica pores with environmentally responsive functional groups (e.g., transferrin) or polymers (e.g., Eudragit) could be investigated.

Moreover, KAZ3 loaded formulations should be further tested in animal models such as tumor xenograft to test their ability to co-deliver anticancer agent and siRNA to the tumor selectively through passive targeting, their gene silencing and cancer cell cytotoxicity should be further tested in *in-vivo* models. Their biodistribution and adverse effects in different body organs should also be assessed to validate true potential, viability and toxicity. Future studies should include a systematic evaluation of biodegradation behaviour under physiologically relevant conditions to fully assess the biosafety profile of the system.

CRediT authorship contribution statement

Elshaimaa Sayed: Validation, Investigation, Formal analysis, Conceptualization, Writing – original draft, Methodology, Funding acquisition, Data curation. Ketan Ruparelia: Writing – review & editing, Methodology, Formal analysis, Software, Investigation. Saman Zafar: Writing – original draft, Methodology, Validation, Formal analysis. Ahmed Faheem: Validation, Writing – review & editing, Formal analysis. Dimitris Fatouros: Validation, Formal analysis, Writing – review & editing, Methodology. Muhammad Sohail Arshad: Validation, Methodology, Conceptualization, Writing – review & editing, Supervision, Formal analysis. Neenu Singh: Writing – review & editing, Supervision, Data curation, Validation, Investigation. Zeeshan Ahmad: Validation, Project administration, Funding acquisition, Conceptualization, Writing – review & editing, Supervision, Investigation, Formal analysis.

Declaration of competing interest

The authors declare that they have no known competing financial interests or personal relationships that could have appeared to influence the work reported in this paper.

Acknowledgement

The authors would like to thankfully acknowledge the Egyptian Culture Centre and the Educational Bureau in London for funding this research. The authors also thank The Royal Society for their support.

Data availability

All data has been presented in the manuscript

References

- [1] J.H. Sun, C. Ye, E.H. Bai, L.L. Zhang, S.J. Huo, H.H. Yu, S.Y. Xiang, S.Q. Yu, Co-delivery nanoparticles of doxorubicin and chloroquine for improving the anticancer effect in vitro, Nanotechnology 30 (2018) 085101, https://doi.org/10.1088/1361-6528/AAF51B.
- [2] Y. Huang, S.P.C. Cole, T. Cai, Y. Cai, Applications of nanoparticle drug delivery systems for the reversal of multidrug resistance in cancer (review), Oncol. Lett. 12 (2016) 11–15.
- [3] E. Sayed, Y. Alyassin, A. Zaman, K. Ruparelia, N. Singh, M.-W. Chang, Z. Ahmad, Porous inorganic nanomaterials for drug delivery, Handb. Mater. Nanomedicine (2020) 295–348, https://doi.org/10.1201/9781003045076-8.
- [4] E. Sayed, R. Haj-Ahmad, K. Ruparelia, M.S. Arshad, M.W. Chang, Z. Ahmad, Porous inorganic drug delivery systems—a review, AAPS PharmSciTech 18 (2017) 1507–1525, https://doi.org/10.1208/S12249-017-0740-2.
- [5] L. Li, W. Gu, J. Chen, W. Chen, Z.P. Xu, Co-delivery of siRNAs and anti-cancer drugs using layered double hydroxide nanoparticles, Biomaterials 35 (2014) 3331–3339, https://doi.org/10.1016/J.BIOMATERIALS.2013.12.095.
- [6] R. Li, Y. Xie, Nanodrug delivery systems for targeting the endogenous tumor microenvironment and simultaneously overcoming multidrug resistance properties, J. Control. Release 251 (2017) 49–67, https://doi.org/10.1016/J. JCONREL 2017 02 020
- [7] L.S. Jabr-Milane, L.E. van Vlerken, S. Yadav, M.M. Amiji, Multi-functional nanocarriers to overcome tumor drug resistance, Cancer Treat. Rev. 34 (2008) 592–602. https://doi.org/10.1016/J.CTRV.2008.04.003.
- [8] Y. Feng, N. Panwar, D.J.H. Tng, S.C. Tjin, K. Wang, K.T. Yong, The application of mesoporous silica nanoparticle family in cancer theranostics, Coord. Chem. Rev. 319 (2016) 86–109, https://doi.org/10.1016/J.CCR.2016.04.019.
- [9] E. Sayed, C. Karavasili, K. Ruparelia, R. Haj-Ahmad, G. Charalambopoulou, T. Steriotis, D. Giasafaki, P. Cox, N. Singh, L.P.N. Giassafaki, A. Mpenekou, C. K. Markopoulou, I.S. Vizirianakis, M.W. Chang, D.G. Fatouros, Z. Ahmad, Electrosprayed mesoporous particles for improved aqueous solubility of a poorly water soluble anticancer agent: in vitro and ex vivo evaluation, J. Control. Release 278 (2018) 142–155, https://doi.org/10.1016/j.jconrel.2018.03.031.
- [10] Y. Alyassin, E.G. Sayed, P. Mehta, K. Ruparelia, M.S. Arshad, M. Rasekh, J. Shepherd, I. Kucuk, P.B. Wilson, N. Singh, M.W. Chang, D.G. Fatouros, Z. Ahmad, Application of mesoporous silica nanoparticles as drug delivery carriers for chemotherapeutic agents, Drug Discov. Today 25 (2020) 1513–1520, https:// doi.org/10.1016/J.DRUDIS.2020.06.006.
- [11] H. Meng, W.X. Mai, H. Zhang, M. Xue, T. Xia, S. Lin, X. Wang, Y. Zhao, Z. Ji, J. I. Zink, A.E. Nel, Codelivery of an optimal drug/siRNA combination using mesoporous silica nanoparticles to overcome drug resistance in breast cancer in vitro and in vivo, ACS Nano 7 (2013) 994–1005, https://doi.org/10.1021/NN3044066/SUPPL_FILE/NN3044066_SI_001.PDF.
- [12] L. Jia, Z. Li, J. Shen, D. Zheng, X. Tian, H. Guo, P. Chang, Multifunctional mesoporous silica nanoparticles mediated co-delivery of paclitaxel and tetrandrine for overcoming multidrug resistance, Int. J. Pharm. 489 (2015) 318–330, https:// doi.org/10.1016/J.IJPHARM.2015.05.010.
- [13] A.M. Chen, M. Zhang, D. Wei, D. Stueber, O. Taratula, T. Minko, H. He, Co-delivery of doxorubicin and Bcl-2 siRNA by mesoporous silica nanoparticles enhances the efficacy of chemotherapy in multidrug-resistant cancer cells, Small 5 (2009) 2673–2677, https://doi.org/10.1002/SMLL.200900621.
- [14] Z. Li, L. Zhang, C. Tang, C. Yin, Co-delivery of doxorubicin and survivin shRNA-expressing plasmid via microenvironment-responsive dendritic mesoporous silica nanoparticles for synergistic cancer therapy, Pharm. Res. 34 (2017) 2829–2841, https://doi.org/10.1007/S11095-017-2264-6/METRICS.
- [15] G. Zheng, R. Zhao, A. Xu, Z. Shen, X. Chen, J. Shao, Co-delivery of sorafenib and siVEGF based on mesoporous silica nanoparticles for ASGPR mediated targeted HCC therapy, Eur. J. Pharm. Sci. 111 (2018) 492–502, https://doi.org/10.1016/J. EUS. 2017.10.036
- [16] J. Shen, H.C. Kim, H. Su, F. Wang, J. Wolfram, D. Kirui, J. Mai, C. Mu, L.N. Ji, Z. W. Mao, H. Shen, Cyclodextrin and polyethylenimine functionalized mesoporous silica nanoparticles for delivery of siRNA cancer therapeutics, Theranostics 4 (2014) 487–497, https://doi.org/10.7150/THNO.8263.
- [17] M. Wang, X. Li, Y. Ma, H. Gu, Endosomal escape kinetics of mesoporous silicabased system for efficient siRNA delivery, Int. J. Pharm. 448 (2013) 51–57, https://doi.org/10.1016/J.IJPHARM.2013.03.022.
- [18] T. Xia, M. Kovochich, M. Liong, H. Meng, S. Kabehie, S. George, J.I. Zink, A.E. Nel, Polyethyleneimine coating enhances the cellular uptake of mesoporous silica nanoparticles and allows safe delivery of siRNA and DNA constructs, ACS Nano 3 (2009) 3273–3286, https://doi.org/10.1021/NN900918W/SUPPL_FILE/ NN900918W SI 002_PDF.
- [19] K. Möller, K. Müller, H. Engelke, C. Bräuchle, E. Wagner, T. Bein, Highly efficient siRNA delivery from core-shell mesoporous silica nanoparticles with multifunctional polymer caps, Nanoscale 8 (2016) 4007–4019, https://doi.org/ 10.1030/CFNIPG246P.
- [20] D. Oupicky, S.R. Bhattarai, E. Muthuswamy, A. Wani, M. Brichacek, A. L. Castañeda, S.L. Brock, Enhanced gene and siRNA delivery by polycation-modified mesoporous silica nanoparticles loaded with chloroquine, Pharm. Res. 27 (2010) 2556–2568, https://doi.org/10.1007/S11095-010-0245-0/METRICS.
- [21] S. Zhang, B. Zhao, H. Jiang, B. Wang, B. Ma, Cationic lipids and polymers mediated vectors for delivery of siRNA, J. Control. Release 123 (2007) 1–10, https://doi.org/ 10.1016/J.JCONREL.2007.07.016.
- [22] G. Shim, M.G. Kim, J.Y. Park, Y.K. Oh, Small interfering RNAs (siRNAs) as cancer therapeutics, Biomater. Cancer Ther. Diagn. Prev. Ther. (2013) 237–269, https:// doi.org/10.1533/9780857096760.3.237.

- [23] Z. Yang, D. Gao, Z. Cao, C. Zhang, D. Cheng, J. Liu, X. Shuai, Drug and gene codelivery systems for cancer treatment, Biomater. Sci. 3 (2015) 1035–1049, https:// doi.org/10.1039/C4BM00369A.
- [24] J.D. Ziebarth, D.R. Kennetz, N.J. Walker, Y. Wang, Structural comparisons of PEI/DNA and PEI/siRNA complexes revealed with molecular dynamics simulations, J. Phys. Chem. B 121 (2017) 1941–1952, https://doi.org/10.1021/ACS. JPCB.6B10775/SUPPL FILE/JP6B10775 SI 001.PDF.
- [25] G. Navarro, S. Essex, R.R. Sawant, S. Biswas, D. Nagesha, S. Sridhar, C.T. de ILarduya, V.P. Torchilin, Phospholipid-modified polyethylenimine-based nanopreparations for siRNA-mediated gene silencing: Implications for transfection and the role of lipid components, Nanomed. Nanotechnol. Biol. Med. 10 (2014) 411–419, https://doi.org/10.1016/J.NANO.2013.07.016.
- [26] P.Y. Teo, C. Yang, J.L. Hedrick, A.C. Engler, D.J. Coady, S. Ghaem-Maghami, A.J. T. George, Y.Y. Yang, Hydrophobic modification of low molecular weight polyethylenimine for improved gene transfection, Biomaterials 34 (2013) 7971–7979, https://doi.org/10.1016/J.BIOMATERIALS.2013.07.005.
- [27] G. Navarro, R.R. Sawant, S. Biswas, S. Essex, C. Tros De Ilarduya, V.P. Torchilin, P-glycoprotein silencing with siRNA delivered by dope-modified pei overcomes doxorubicin resistance in breast cancer cells, Nanomedicine 7 (2012) 65–78, https://doi.org/10.2217/NNM.11.93.
- [28] S. Essex, G. Navarro, P. Sabhachandani, A. Chordia, M. Trivedi, S. Movassaghian, V.P. Torchilin, Phospholipid-modified PEI-based nanocarriers for in vivo siRNA therapeutics against multidrug-resistant tumors, Gene Ther. 22 (2014) 257–266, https://doi.org/10.1038/gt.2014.97.
- [29] A. Ali, A. Zaman, E. Sayed, D. Evans, S. Morgan, C. Samwell, J. Hall, M.S. Arshad, N. Singh, O. Qutachi, M.W. Chang, Z. Ahmad, Electrohydrodynamic atomisation driven design and engineering of opportunistic particulate systems for applications in drug delivery, therapeutics and pharmaceutics, Adv. Drug Deliv. Rev. 176 (2021) 113788, https://doi.org/10.1016/j.addr.2021.04.026.
- [30] P. Mehta, M. Rasekh, M. Patel, E. Onaiwu, K. Nazari, I. Kucuk, P.B. Wilson, M. S. Arshad, Z. Ahmad, M.W. Chang, Recent applications of electrical, centrifugal, and pressurised emerging technologies for fibrous structure engineering in drug delivery, regenerative medicine and theranostics, Adv. Drug Deliv. Rev. 175 (2021) 113823, https://doi.org/10.1016/j.addr.2021.05.033.
- [31] J.C. Wang, M.W. Chang, Z. Ahmad, J.S. Li, Fabrication of patterned polymerantibiotic composite fibers via electrohydrodynamic (EHD) printing, J. Drug Deliv. Sci. Technol. 35 (2016) 114–123, https://doi.org/10.1016/j.jddst.2016.06.009.
- [32] Z.C. Yao, S.C. Chen, Z. Ahmad, J. Huang, M.W. Chang, J.S. Li, Essential oil bioactive fibrous membranes prepared via coaxial electrospinning, J. Food Sci. 82 (2017) 1412–1422, https://doi.org/10.1111/1750-3841.13723.
- [33] M. Nangrejo, Z. Ahmad, E. Stride, M. Edirisinghe, P. Colombo, Preparation of polymeric and ceramic porous capsules by a novel electrohydrodynamic process, Pharm. Dev. Technol. 13 (2008) 425–432, https://doi.org/10.1080/ 10837450802247929
- [34] Z. Ahmad, E. Stride, M. Edirisinghe, Novel preparation of transdermal drugdelivery patches and functional wound healing materials, J. Drug Target. 17 (2009) 724–729, https://doi.org/10.3109/10611860903085386.
- [35] P. Toman, C.F. Lien, Z. Ahmad, S. Dietrich, J.R. Smith, Q. An, É. Molnár, G. J. Pilkington, D.C. Górecki, J. Tsibouklis, E. Barbu, Nanoparticles of alkylglyceryl-dextran-graft-poly(lactic acid) for drug delivery to the brain: preparation and in vitro investigation, Acta Biomater. 23 (2015) 250–262, https://doi.org/10.1016/j.actbio.2015.05.009.
- [36] P. Mehta, A.A. Al-Kinani, M.S. Arshad, M.W. Chang, R.G. Alany, Z. Ahmad, Development and characterisation of electrospun timolol maleate-loaded polymeric contact lens coatings containing various permeation enhancers, Int. J. Pharm. 532 (2017) 408–420, https://doi.org/10.1016/J.IJPHARM.2017.09.029.
 [37] P. Mehta, A.A. Al-Kinani, M.S. Arshad, N. Singh, S.M. van der Merwe, M.W. Chang,
- [37] P. Menta, A.A. Al-Kinani, M.S. Arshad, N. Singh, S.M. van der Merwe, M.W. Chang R.G. Alany, Z. Ahmad, Engineering and development of chitosan-based nanocoatings for ocular contact lenses, J. Pharm. Sci. 108 (2019) 1540–1551, https://doi.org/10.1016/j.xphs.2018.11.036.
- [38] A. Ali, S. Zafar, M. Rasekh, T.A. Chohan, F. Pisapia, N. Singh, O. Qutachi, M. S. Arshad, Z. Ahmad, An adaptive approach in polymer-drug nanoparticle engineering using slanted electrohydrodynamic needles and horizontal spraying planes, AAPS PharmSciTech 25 (2024) 257, https://doi.org/10.1208/S12249-024-02971-Y/METRICS.
- [39] M. Enayati, Z. Ahmad, E. Stride, M. Edirisinghe, Preparation of polymeric carriers for drug delivery with different shape and size using an electric jet, Curr. Pharm. Biotechnol. 10 (2009) 600–608, https://doi.org/10.2174/138920109789069323.
- [40] Z. Ekemen, Z. Ahmad, E. Stride, D. Kaplan, M. Edirisinghe, Electrohydrodynamic bubbling: an alternative route to fabricate porous structures of silk fibroin based materials, Biomacromolecules 14 (2013) 1412–1422, https://doi.org/10.1021/ BM400068K/ASSET/IMAGES/MEDIUM/BM-2013-00068K_0012.GIF.
- [41] D.M. Yunos, Z. Ahmad, A.R. Boccaccinia, Fabrication and characterization of electrospun poly-DL-lactide (PDLLA) fibrous coatings on 45S5 Bioglass® substrates for bone tissue engineering applications, J. Chem. Technol. Biotechnol. 85 (2010) 768–774, https://doi.org/10.1002/jctb.2283.
- [42] Y. Gao, M.W. Chang, Z. Ahmad, J.S. Li, Magnetic-responsive microparticles with customized porosity for drug delivery, RSC Adv. 6 (2016) 88157–88167, https:// doi.org/10.1039/c6ra17162a.
- [43] Z. Ahmad, E.S. Thian, J. Huang, M.J. Edirisinghe, S.M. Best, S.N. Jayasinghe, W. Bonfield, R.A. Brooks, N. Rushton, Deposition of nano-hydroxyapatite particles utilising direct and transitional electrohydrodynamic processes, J. Mater. Sci. Mater. Med. 19 (2008) 3093–3104, https://doi.org/10.1007/s10856-008-3436-z.
- [44] J.C. Wang, H. Zheng, M.W. Chang, Z. Ahmad, J.S. Li, Preparation of active 3D film patches via aligned fiber electrohydrodynamic (EHD) printing, Sci. Rep. 7 (2017) 1–13, https://doi.org/10.1038/srep43924.

- [45] S. Wu, Z. Ahmad, J.S. Li, M.W. Chang, Fabrication of flexible composite drug films via foldable linkages using electrohydrodynamic printing, Mater. Sci. Eng. C 108 (2020) 110393, https://doi.org/10.1016/J.MSEC.2019.110393.
- [46] S. Zafar, E. Sayed, S.J. Rana, M. Rasekh, E. Onaiwu, K. Nazari, I. Kucuk, D. G. Fatouros, M.S. Arshad, Z. Ahmad, Particulate atomisation design methods for the development and engineering of advanced drug delivery systems: a review, Int. J. Pharm. 666 (2024) 124771, https://doi.org/10.1016/J.JJPHARM.2024.124771.
- [47] N. Ellis, C.U. Yurteri, J. Ruud van Ommen, Continuous process to deposit nanoparticles onto microparticles, Chem. Eng. J. 181–182 (2012) 798–805, https://doi.org/10.1016/J.CEJ.2011.11.102.
- [48] M.Y. Hanafi-Bojd, M.R. Jaafari, N. Ramezanian, M. Xue, M. Amin, N. Shahtahmassebi, B. Malaekeh-Nikouei, Surface functionalized mesoporous silica nanoparticles as an effective carrier for epirubicin delivery to cancer cells, Eur. J. Pharm. Biopharm. 89 (2015) 248–258, https://doi.org/10.1016/J. E.JPB.2014.12.009.
- [49] M. Jin, D.G. Yu, C.F.G.C. Geraldes, G.R. Williams, S.W.A. Bligh, Theranostic fibers for simultaneous imaging and drug delivery, Mol. Pharm. 13 (2016) 2457–2465, https://doi.org/10.1021/ACS.MOLPHARMACEUT.6B00197/SUPPL_FILE/ MP6B00197 SI 001.PDF.
- [50] Y. Zhang, Z. Zhi, T. Jiang, J. Zhang, Z. Wang, S. Wang, Spherical mesoporous silica nanoparticles for loading and release of the poorly water-soluble drug telmisartan, J. Control. Release 145 (2010) 257–263, https://doi.org/10.1016/J. JCONREL 2010 04 029
- [51] N. Miriyala, D. Ouyang, Y. Perrie, D. Lowry, D.J. Kirby, Activated carbon as a carrier for amorphous drug delivery: effect of drug characteristics and carrier wettability, Eur. J. Pharm. Biopharm. 115 (2017) 197–205, https://doi.org/ 10.1016/J.EJPB.2017.03.002.

- [52] S. Hong, S. Shen, D.C.T. Tan, W.K. Ng, X. Liu, L.S.O. Chia, A.W. Irwan, R. Tan, S. A. Nowak, K. Marsh, R. Gokhale, High drug load, stable, manufacturable and bioavailable fenofibrate formulations in mesoporous silica: a comparison of spray drying versus solvent impregnation methods, Drug Deliv. 23 (2016) 316–327, https://doi.org/10.3109/10717544.2014.913323.
- [53] C.S. Thompson, R.A. Fleming, M. Zou, Transparent self-cleaning and antifogging silica nanoparticle films, Sol. Energy Mater. Sol. Cells 115 (2013) 108–113, https://doi.org/10.1016/J.SOLMAT.2013.03.030.
- [54] Y. Hu, A. Bouamrani, E. Tasciotti, L. Li, X. Liu, M. Ferrari, Tailoring of the nanotexture of mesoporous silica films and their functionalized derivatives for selectively harvesting low molecular weight protein, ACS Nano 4 (2010) 439–451, https://doi.org/10.1021/NN901322D/SUPPL_FILE/NN901322D_SI_001.PDF.
- [55] T. Sun, Y. Sun, H. Zhang, Phospholipid-coated mesoporous silica nanoparticles acting as lubricating drug nanocarriers, Polymers (basel). 10 (2018) 513, https://doi.org/10.3390/POLYM10050513.
- [56] A.E. Nel, H. Meng, X. Liu, US10143660B2 Mesoporous silica nanoparticles with lipid bilayer coating for cargo delivery, Google Patents (2018). https://patents. google.com/patent/US10143660B2/en (accessed February 5, 2025).
- [57] T.J. McIntosh, Hydration properties of lamellar and non-lamellar phases of phosphatidylcholine and phosphatidylethanolamine, Chem. Phys. Lipids 81 (1996) 117–131, https://doi.org/10.1016/0009-3084(96)02577-7.
- [58] M.H. Teixeira, G.M. Arantes, Effects of lipid composition on membrane distribution and permeability of natural quinones, RSC Adv. 9 (2019) 16892–16899, https://doi.org/10.1039/C9RA01681C.
- [59] C.F. Wang, Y.X. Lin, T. Jiang, F. He, R.X. Zhuo, Polyethylenimine-grafted polycarbonates as biodegradable polycations for gene delivery, Biomaterials 30 (2009) 4824–4832, https://doi.org/10.1016/J.BIOMATERIALS.2009.05.053.